FINAL REPORT FOR THE PROJECT ENTITLED "AN ACCELERATOR-BASED NEUTRON SOURCE FOR BNCT"

Contract No. DE-FG02-93ER61612

THE OHIO STATE UNIVERSITY

PRINCIPAL INVESTIGATORS:

THOMAS E. BLUE

KAMBIZ VAFAI

REINHARD GAHBAUER

MECHANICAL ENGINEERING DEPARTMENT

THE OHIO STATE UNIVERSITY

206 WEST 18TH AVE, COLUMBUS, OHIO 43210

March 2006

TABLE OF CONTENTS FOR FINAL REPORT

Introduction 1

Background 3

Accomplishments 7

1. Neutronics and Moderator Assembly Design 7

1.1. Calculational Studies 7

1.1.1. Neutron RBE Sensitivity Analysis

1.1.2. In-Phantom Beam Assessment Parameters

1.1.3. Moderator Assembly Optimization Analysis-Phase 1

1.1.4. Moderator Assembly Optimization Analysis-Phase 2

1.1.5 Delimiter Design Using MIRD and Zubal Phantoms

1.1.5.1 Patient Phantoms

1.1.5.1.1 Zubal Phantom

1.1.5.1.2 MIRD Phantom

1.1.5.2 Model Geometry

1.1.5.3 Results

1.2. Experimental Studies-Moderator Assembly Experimental Verification 22

1.2.1. Bare Target Measurements

1.2.1.1. Proton Recoil Measurements

1.2.1.2. Paired Ion Chamber Measurements

1.2.2. Moderator Assembly Measurements

1.2.2.1. In-Air Measurements

1.2.2.2. In-Phantom Measurements

2. Thermal-Hydraulics and Target Assembly Design 35

2.1 Overview 35

2.2 Calculational Studies of Microchannel HRS 37

2.3 Experimental Studies of Microchannel HRS 43

2.3.1 Microchannel Pressure Drop Experiment

2.3.2 Microchannel Heat Transfer Coefficient Experiment

References for Final Report 47

Graduate Degrees Earned 51

Project Related Publications 53

INTRODUCTION

Boron Neutron Capture Therapy (BNCT)

The overall objective of our research project is to develop an Accelerator-based Epithermal Neutron Irradiation Facility (AENIF) for Boron Neutron Capture Therapy (BNCT). Specifically, our goals were to design, and confirm by measurement, a target assembly and a moderator assembly which fulfill the design requirements of the ABNS. The design requirements were: 1) that the neutron field quality be as good as the neutron field quality for the Brookhaven Medical Research Reactor (BMRR)(this requirement evolved over time to be that the neutron field quality be as good as the neutron field quality for the Massachusetts Institute of Technology (MIT) epithermal neutron field for BNCT at the MIT Research Reactor (MITR) ; 2) that the patient treatment time be reasonable; 3) that the proton current required to treat patients in reasonable times be technologically achievable at a reasonable cost with good reliability, and with an accelerator that has space requirements which can be met in a hospital environment; and finally 4) that the treatment be safe for the patients with respect to the accelerator, target assembly and moderator assembly.

BNCT is an experimental radiation therapy modality for the treatment of highly malignant tumors that are resistant to other treatment modalities. It is based upon the $^{10}B(n,\square)^{7}Li$ reaction. In BNCT, compounds which contain ^{10}B (a non-radioactive isotope of boron which occurs in nature and comprises approximately 20% of elemental boron) are administered to the patient. These compounds carry boron to the tumor, where it attaches to or is incorporated within the tumor cells. Then the tumor site is irradiated with neutrons. The neutrons are absorbed by the ^{10}B, producing short range (about a cell diameter) high linear energy transfer (LET) ^{4}He and ^{7}Li nuclei, which selectively destroy malignant cells that contain a sufficient amount of ^{10}B [1,2]. Normal tissues adjacent to the tumor are spared if their boron concentration is low.

BNCT can be thought of as a form of chemotherapy, for which the action of the chemo-therapeutic agent is restricted to those portions of the body where there are both neutrons and boron. The binary nature of BNCT offers a significant advantage over conventional chemotherapy, in that the action of compounds of boron, which localize in normal tissues (such as the liver, kidneys, and spleen), as well as in the tumor, are restricted to those regions of the patients body which are irradiated by neutrons. For

example, if BNCT were used to treat non-metastatic tumors of the brain, a compound which localized boron in the liver, as well as in the tumor, would be potentially useful, since a patients' head could be irradiated with neutrons without exposing the liver to a large fluence of neutrons.

As a binary therapy, the requirements for successful treatment of malignant tumors by BNCT are (1) a boronated compound which localizes with good specificity in the tumor (i.e. specifically in the tumor, but not in the adjacent normal tissue) in concentrations greater than approximately 30 μg ^{10}B/g tumor, and (2) a neutron irradiation facility with a neutron flux which is large enough so that a patient can be treated in less than about one-half hour with a single fraction of a fractionated dose regimen.

Scientific Rationale for an AENIF

Presently a patient who is diagnosed with a glioma has very little hope for long term survival [3]. The pattern of growth of gliomas is such that their complete surgical removal is almost always impossible. Furthermore they respond poorly to both chemotherapy and conventional radiotherapy. Presently, approximately 11,000 individuals are diagnosed with gliomas annually [4]. For BNCT to be widely applied to the treatment of refractory tumors, such as gliomas, sources of neutrons must be widely available. There are relatively few research reactors with adequate power and siting close enough to a major research hospital, for the reactors to be useful for BNCT. Therefore, accelerator-based sources of neutrons must be available, if BNCT is to be widely used. Also, methods of administration of boronated compounds can be used in a hospital environment (such as intra-arterial administration preceded by blood–brain barrier disruption) that cannot be safely employed in a reactor environment. These methods of administration may increase the therapeutic efficacy of the boronated compounds.

Major Components of an AENIF for BNCT and Scope of Project

The major components of an AENIF for BNCT are 1) an accelerator-based neutron source consisting of a high-current low-energy proton accelerator, a high-energy beam transport system, a target assembly, and a moderator assembly and 2) a suitable

facility structure consisting of an accelerator room, a treatment room, a control room, and rooms for patient preparation and care, as well as rooms for faculty and staff.

During the course of this project, we have designed an AENIF for BNCT, and demonstrated by calculations that an AENIF, for the treatment of gliomas by BNCT is feasible, for a 10 mA, 2.5 MeV proton beam. Using first the Ohio State University (OSU) Van de Graaff accelerator with a simple D_2O moderator assembly, and then the Ohio University (OU) Van de Graaff accelerator with a simple D_2O moderator assembly, we have confirmed our neutronic calculations, by measurements in air [5,6,7], by measurements in rectangular parallelepiped water phantoms [8,9,10], and by measurements in ellipsoidal methylmethacrylate phantoms. Also, we have designed a disk-shaped heat pipe target assembly and designed, and tested the design, of a rectangular micro-channel target assembly. We have established that the micro-channel target assembly can remove, without exceeding the melting temperature of lithium, the 25 kW of beam power of a 10 mA beam [11,12], if the beam power is distributed over the surface of a 25 cm diameter target, by a high energy beam transport system that we have designed.

BACKGROUND

A More Detailed Description of the AENIF Design

The accelerator produces a high current (10mA) beam of 2.5 MeV protons. The protons are transported to a ^7Li target by a high-energy beam transport system. Neutrons are generated when the beam protons strike the target. The neutrons which are generated in the target are too energetic to be directly used for BNCT, and are therefore moderated (reduced in energy) by the moderator assembly as they traverse the moderator assembly to the patient.

Figure 1 shows a schematic diagram of the accelerator, the high-energy beam transport system, the target assembly, and the moderator assembly [13]

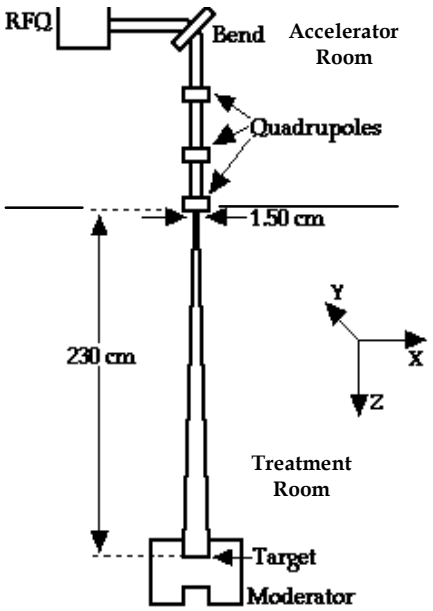

Fig. 1: The accelerator, beam transport system (approx. to scale)

Two configurations have been analyzed, a vertical configuration and a horizontal configuration. For the vertical configuration, the beam transport system directs the proton beam vertically downward out of the ceiling, so that the target is horizontal. With this configuration, if the target melts, the lithium will not flow out of the beam spot (i.e. that spot where the target assembly is irradiated). For the horizontal configuration, the beam transport system directs the proton beam horizontally through a 90 degree bend and the beam enters the treatment room through a side-wall. In this configuration, the target is vertical. If the target melts, or slumps, the lithium will flow out of the beam spot. For purposes of target heat removal, the beam transport system spreads the beam to a diameter of 25 cm at the target, resulting in an average power deposition per unit area on the target of approximately 0.6 MW/m^2, for a 10mA proton beam current of 2.5 MeV protons, and a peak heat flux of 1.6 MW/m^2 with a peak to average heat flux ratio of 3.1.

For the vertical configuration, the facility structure must have two levels. The accelerator room is located on the upper level. It contains the accelerator, and the beam-line magnets. The treatment room is located on the lower level. It contains the target assembly and the portion of the beam line that is below the last magnet. The shielding which is necessary for the radiological protection of the staff has been calculated for both the vertical and the horizontal configurations.

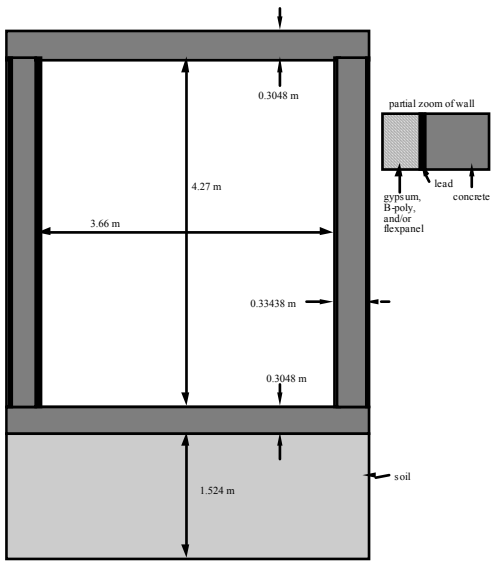

Fig. 2: A side-view of treatment room.

Figure 2 presents a side view of the treatment room for the vertical configuration. For the vertical configuration, we have conservatively calculated that, if the concrete walls of the treatment room are 1.8m thick, then facility personnel will be adequately protected from excessive radiation exposure [14].

As shown in Fig. 1, the HEBT system consists of bending and focusing magnets and a drift tube through which the protons stream. For the vertical configuration, the drift tube will penetrate the ceiling separating the accelerator room from the treatment room. The treatment room will house the moderator assembly and, of course, the target assembly. Target thermal design considerations affect the HEBT system design through the thermal design requirement that the proton beam power be distributed as uniformly as possible in space and in time over a large diameter. Considerations regarding the shielding of the accelerator room, also directly affect the HEBT system design, since neutron activation of the accelerator and the HEBT system magnets should be minimized. This can be accomplished by placing a bend in the beam line. Also, the large target diameter demanded by the target thermal design can be used to advantage in the HEBT system shielding design, if the HEBT system brings the beam through a narrow pinch as it enters the treatment room. Then the number of neutrons entering the accelerator room from the treatment room is minimized, because the solid angle subtended by the HEBT is small for a neutron born in the target.

A graduate research assistant (Mr. Michael Christian Dobelbower, now Dr. Michael Christian Dobelbower, M.D., Ph.D.) spent the month of January, 1994 working at Los Alamos National Laboratory with the staff of the AT-1 Division. There he learned to run the HEBT design code PARMILA, which he brought back to OSU. He designed two HEBT systems [15]. For specificity, he assumed input parameters for the HEBT system design which are consistent with the output of an RFQ. One HEBT system uses static magnetic fields to spread the beam uniformly (the power peaking factor equals ~1.4) over a 25 cm diameter target. A second lower cost, less uniform HEBT system, statically spreads the beam over a 25 cm diameter target and includes a 90° bend in the beam line. The results of Dr. Dobelower's work for the lower cost transport system is described in more detail below. It is the HEBT system which is shown in Fig. 1 above. It consists of a bending magnet and 3 quadrupole magnets. Some important characteristics of the various magnets and beam transport elements are shown in Table 1.

Table 1: "Non-uniform" Beam Line Elements

Element	Effective Length (cm)	Aperture Radius (cm)	Gradient	Pole Tip Field (G)
Drift	10	3.5		
Bend	3			
Drift	10	3.5		
Quad. 1	10	5	–1700 G/cm	-8500
Drift	22	10		
Quad. 2	10	5	1780 G/cm	8900
Drift	8	5		
Quad. 3	15	2.5	–2000 G/cm	-5000
Drift	290	15		
Total	378			

The low-cost beam transport system begins with a bending magnet. The function of the bending magnet is to alter the path of the beam so that the RFQ is not in the backshine of neutrons from the target assembly. The next three magnets in the beamline are quadrupoles that are used to focus the beam through a pinch point to a 25-cm diameter circle at the lithium target. As mentioned previously, this pinch point presents a small solid angle to neutrons born in the 25 cm diameter lithium target, and greatly reduces the number of neutron streaming from the treatment room back into the accelerator room.

A graph of the beam envelope vs. distance along the beam-line is shown in Fig. 5. The calculated peak heat flux for a 10 mA beam of 2.5 MeV protons was calculated to be

1.6 MW/m^2 with a peak to average heat flux ratio of 3.1. The overall transport length of the "non-uniform" beam transport system is 378 cm.

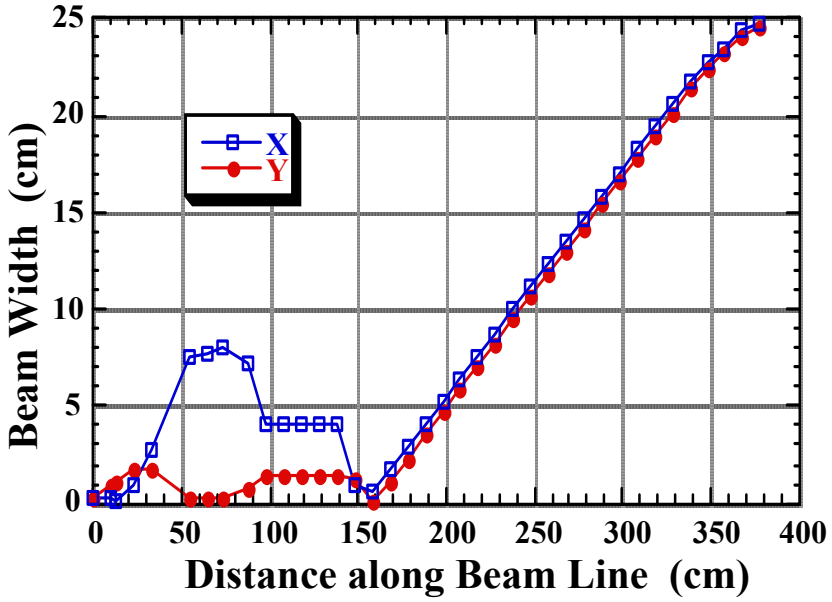

Fig. 3: Beam envelope for "non-uniform beam system.

ACCOMPLISHMENTS

Accomplishments with respect to the Shielding and High Energy Beam Transport System Designs have been discussed above and will not be discussed further. Other accomplishments are discussed below.

1. NEUTRONICS AND MODERATOR ASSEMBLY DESIGN

1.1 Calculational Studies

Over the project period, we have developed and refined our calculational capabilities. These include: 1) development of an energy dependent normal tissue neutron RBE; 2) development of in-phantom neutron field assessment parameters; 3) in-phantom moderator assembly optimization calculations using the MIRD phantom; and 4) in-phantom moderator assembly optimization calculations using the Zubal head phantom.

1.1.1. Neutron RBE Sensitivity Analysis

We developed an expression for the energy dependent neutron RBE, $RBE(E_n)$ [16]. This expression is based on proton fluence energy distributions resulting from protons born via the $^{14}N(n,p)^{14}C$ and $^{1}H(n,n')^{1}H$ reactions in an infinite tissue medium and an empirical relationship between proton RBE and LET. The expression for $RBE(E_n)$ is presented in Eqn 1.

$$RBE(E_n) = \frac{\int_0^{\infty} \left[\Sigma_s^H(E_n) \left(1 - \frac{E_p}{E_n} \right) \left\{ H(E_p) - H\left(E_p - E_n\right) \right\} + \Sigma_a^N(E_n) \left\{ H(E_p) - H(E_p - E_p^N) \right\} \right] RBE\left(L = \left\langle -\frac{dE}{dx} \right\rangle_{E_p} \right) dE_p}{\left[\Sigma_s^H(E_n) \frac{E_n}{2} + \Sigma_a^N(E_n) E_p^N \right]} \quad (1)$$

where

E_p = the proton energy (keV)

E_n = the neutron energy (keV)

$\mathbf{E_p^N}$ = the energy of a proton from the $^{14}N(n,p)^{14}C$ reaction when the reaction is induced by thermal neutrons (keV)

$\Sigma_s^H(\mathbf{E_n})$ = the energy dependent macroscopic scattering cross section for the $^{1}H(n,n')^{1}H$ reaction (cm^{-1})

$\Sigma_a^N(\mathbf{E_n})$ = the energy dependent macroscopic absorption cross section for the $^{14}N(n,p)^{14}C$ reaction (cm^{-1})

$\left\{ L = \left\langle -\frac{dE}{dx} \right\rangle_{E_p} \right\}$ = the proton LET evaluated at proton energy E_p (keV/μm)

$\mathrm{RBE}\left(L = \left\langle -\frac{dE}{dx} \right\rangle \Big|_{E_p} \right)$ = proton RBE evaluated at a value of LET which is in turn evaluated at E_p

and H(x) = the unit step function, defined as

$$H(x) = \begin{cases} 0 & \text{for } x < 0 \\ 1 & \text{for } x \geq 0 \end{cases}$$

We normalized the RBE for brain such that the absorbed dose averaged RBE, $\langle \mathrm{RBE}^{B}(E_n) \rangle$, was equal to 3.3, the value of the neutron RBE reported by Gavin for the BMRR epithermal neutron beam for the endpoint of late changes in the magnetic resonance images of dogs brains [17]. $\langle \mathrm{RBE}^{B}(E_n) \rangle$ was calculated using neutron kerma factors for brain tissue [18] and the BMRR neutron flux spectrum at the depth of maximum RBE-dose in a dog head phantom. The normalized neutron RBE in adult brain tissue, $\mathrm{RBE}^{B}_{norm}(E_n)$, versus neutron energy is presented in Figure 4.

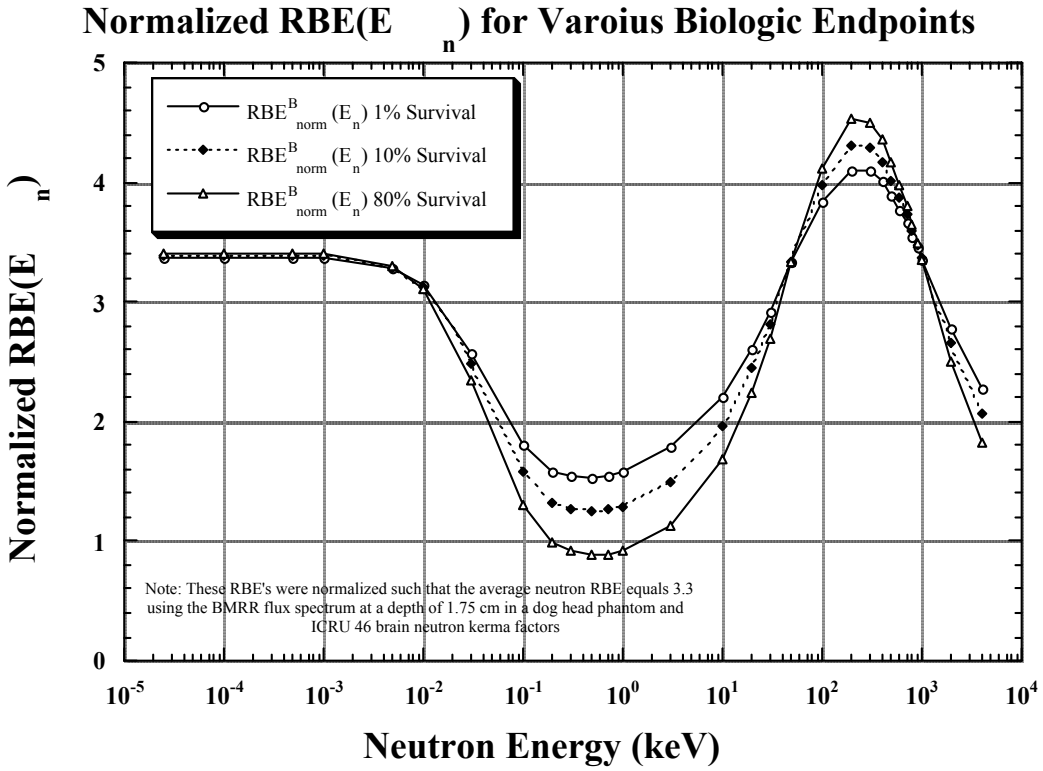

Figure 4: Three curves of the normalized RBE(E_n), $RBE^B_{norm}(E_n)$, versus neutron energy (in keV). Each curve is for $RBE^B_{norm}(E_n)$ calculated using a different biological endpoint.

Then we investigated the effects of biological endpoint on RBE(E_n). Specifically, we calculated the RBE-dose as a function of depth in an ellipsoidal head phantom for each of the three curves of RBE shown in Figure 1, using the neutron flux as a function of depth in phantom for our heavy water moderated accelerator-based neutron source [19]. The resulting RBE-dose depth curves showed that the calculation of the RBE-dose is insensitive to the assumed level of cell-survival, thus showing the robustness of our calculations.

1.1.2. In-Phantom Beam Assessment Parameters

The design of neutron fields for Boron Neutron Capture Therapy (BNCT) is evolving from being based on neutron field parameters in air to being based on neutron field parameters in head phantoms. As a result of this evolution we have developed in-phantom neutron field assessment parameters for evaluation of epithermal neutron fields for use in BNCT. The parameters that we optimize incorporate predicted biological effects in patients' heads. They are based on an energy-spectrum-dependent neutron

normal-tissue RBE and the treatment planning methodology of Gahbauer and his co-workers [20], which includes the effects of dose fractionation.

The first beam assessment parameter is the treatment time, T, and is the total time required for the BNCT treatment. The second beam assessment parameter is the high-LET tumor absorbed-dose, denoted as D_{Tumor}. D_{Tumor} is the product of the high-LET absorbed-dose rate at the tumor location and the calculated treatment time

1.1.3. Moderator Assembly Optimization Analysis-Phase 1

In order for the project to progress in a timely manner, we built a moderator assembly on the basis of an in-air assessment of the moderator assembly performance. Then, we re-assessed the moderator assembly design on the basis of in-phantom beam assessment parameters. This in-phantom assessment generally confirmed the in-air design. Since the in-phantom optimization analysis is based on parameters measured inside a head phantom, this analysis considered irradiation from the superior aspect, as well as lateral irradiations. This subsection describes our in-phantom assessment.

We re-assessed the moderator assemblies on the basis of the in-phantom neutron field assessment parameters, T and D_{Tumor}. A complete discussion of the in-phantom neutron field assessment parameters is provided in reference [19]. For this analysis, the moderator assembly design presented in Figure 5 was used as a starting point and several different moderator/reflector material combinations and moderator thicknesses (denoted as x in the figure) were considered. For each combination, the in-phantom neutron field assessment parameters, T and D_{Tumor}, were calculated. The best moderator assembly for use in our ABNS for BNCT was then selected, from those evaluated, on the basis of the calculated in-phantom neutron field assessment parameters.

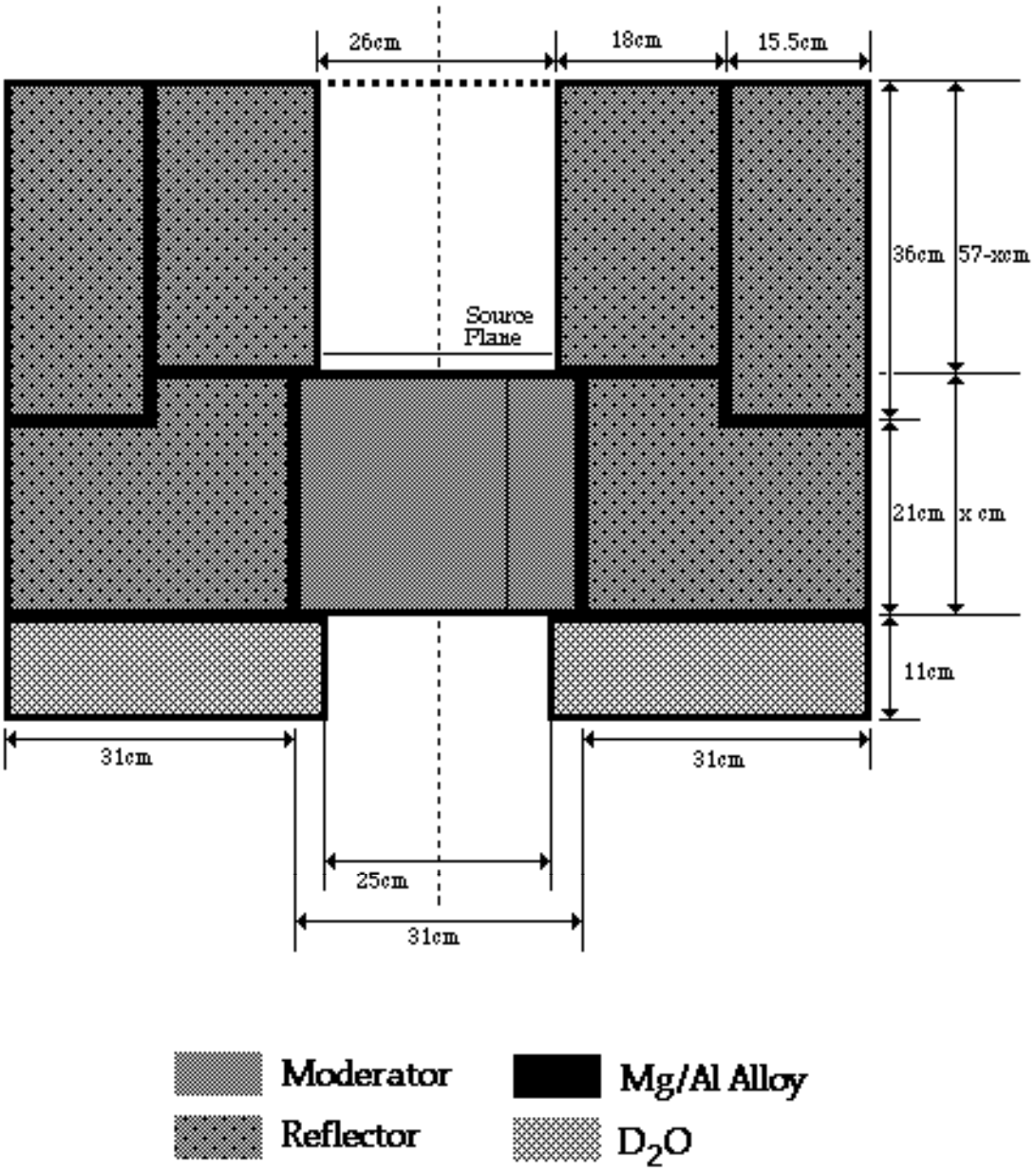

Figure 5. A cross sectional view of the MCNP moderator assembly model used in the moderator assembly analysis. All of the moderator assembly pieces are encased in a 0.5 cm thick Mg/Al alloy shell. Additionally, the front face of the moderator and beam delimiter are coated with a thin layer of ^{6}LiF.

Several different irradiation geometries were considered in this analysis. Specifically, the in-phantom neutron field assessment parameters were calculated for each moderator/reflector combination for a single irradiation from the superior aspect, a

single irradiation from the lateral aspect and a bilateral irradiation. In addition, the effect of different ^{10}B delivery agents (BSH and BPA) on the selection of the optimal assembly was investigated. It should be pointed out that this optimization analysis only considered different moderator and reflector materials and moderator thicknesses. The moderator diameter, reflector dimensions, delimiter and structural material remained the same throughout the analysis.

The moderator/reflector material combinations evaluated in this analysis were: a D_2O moderator with a Li_2CO_3 reflector (D_2O - Li_2CO_3), a D_2O moderator with a MgO reflector (D_2O - MgO), a D_2O moderator with a Pb reflector (D_2O - Pb), a BeO moderator with a Li_2CO_3 reflector (BeO - Li_2CO_3) and a BeO moderator with a MgO reflector (BeO - MgO). For each moderator/reflector material combination, four moderator thicknesses were evaluated; 15 cm, 20 cm, 25 cm and 30 cm.

To perform the analysis, the Monte-Carlo code MCNP4A [22] was used. Moderator assemblies were modeled in MCNP4A and the code was used to calculate the neutron, gamma and specific ^{10}B absorbed dose rates and the kerma averaged RBE, $\overline{RBE(E_n)}_{norm}$, as a function of depth in an ellipsoidal head phantom. These values were then used to calculate the in-phantom neutron field assessment parameters T and D_{Tumor}.

The evaluation of T and D_{Tumor} required that some assumptions were made about the tolerance doses for brain, the treatment fractionation scheme and the boron concentrations and localizations. For this analysis, it was assumed that the patient was treated with four fractions (m=4), in five days. For calculations with BSH as the ^{10}B delivery agent, we assumed the blood boron concentration ([B]) = 30 ppm and the tumor to blood boron concentration ratio ($R_{t/b}$)= 1.3, values typical for the ^{10}B delivery agent BSH [23]. Also, according to an evaluation of the BMRR dog data, for BSH the product of the RBE and compound factor (RBE_BCF) is 0.27 for the endpoint of late changes in the magnetic resonance images of dog's brains [17]. For calculations with BPA as the ^{10}B delivery agent, we assumed [B] = 15 ppm and $R_{t/b}$ = 3.5 [24]. Also, according to a recent evaluation of the BMRR dog data for BPA, the product of RBE_BCF is 1.1 for the endpoint of late changes in the magnetic resonance images of dog's brains [17].

The point of view which we have adopted in designing an ABNS for BNCT is that glioblastoma multiforme is a whole-brain disease, and that recurrences are most likely to arise in the tumor margins that receive the least dose. For a bilateral irradiation,

this corresponds to the midline of the brain, and hence in designing an ABNS for BNCT, we have considered the value of D_{Tumor} at the phantom midline to be most important. Our point of view was that the moderator assembly that provides the highest dose to tumor at the phantom midline, while maintaining a reasonable treatment time, is the best moderator assembly for use in our ABNS for BNCT for the specified treatment parameters.

To assist in the selection of the best moderator assembly, we have plotted D_{Tumor} at the phantom midline versus T, for each moderator assembly and irradiation geometry. As an example, Figures 3 presents a plot of D_{Tumor} (cGy) at the phantom midline versus the treatment time, T (min), for each moderator assembly and moderator thickness, for a single irradiation from the superior aspect, for BSH as the ^{10}B delivery agent. In this analysis, we have assumed that a 10 mA proton beam current is incident on the target of the ABNS. Increasing the proton beam current on the target will proportionately decrease the treatment time.

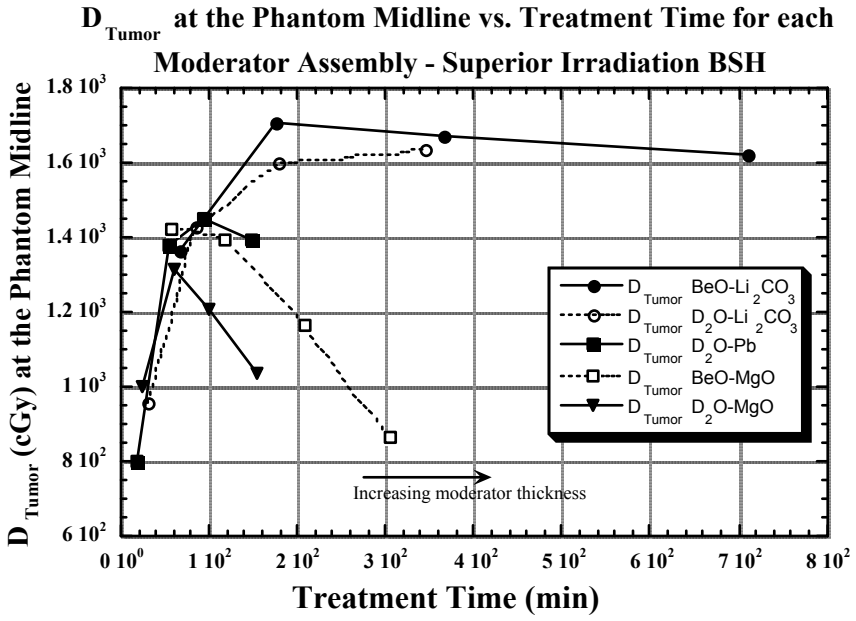

Figure 6. A plot of D_{Tumor} (cGy) at the phantom midline versus the treatment time, T (min), for each moderator assembly and moderator thickness, for a single irradiation from the superior aspect, and BSH as the B-10 delivery agent. Four moderator thicknesses were considered for each moderator assembly (15 cm, 20 cm, 25 cm, and 30 cm). Thinner moderators correspond to shorter treatment times.

We concluded from our analysis that the BeO-Li_2CO_3 moderator assemblies generally provide the largest values of D_{Tumor} at the phantom midline. Based on these plots, the BeO-Li_2CO_3 moderator assembly, with a 20 cm thick BeO moderator, would be the best moderator assembly for use in our ABNS for BNCT, for either BPA or BSH as the delivery agent. Of the limited set of moderator assemblies that we considered we concluded that the D_2O-Li_2CO_3 moderator assembly with a 25 cm thick D_2O moderator is second best to the BeO-Li_2CO_3 moderator assembly. This is fortunate, since we built a D_2O-Li_2CO_3 moderator assembly, due to the unavailability of BeO, as a moderator assembly material.

1.1.4. Moderator Assembly Optimization Analysis-Phase 2

We reevaluated the OSU-ABNS moderator assembly base design for various choices of the moderator assembly materials using the in-phantom neutron field assessment parameters, T and $D_{tumor,6cm}$. Our reevaluation was motivated by the use of Fluental as a moderator material for moderator assemblies for reactor-based neutron sources.

Our reevaluation proceeded in four steps. The first three of these steps are described in this section. The fourth step is described in the following section. In the first step, we re-evaluated the moderator assembly materials on the basis of T and $D_{tumor,6cm}$ in the manner described above. The goals of the moderator assembly design were to maximize $D_{tumor,6cm}$ while maintaining T below 30 minutes per fraction for a four fraction treatment plan with a 10 mA proton beam. This re-evaluation lead to the moderator assembly design that is shown in axial-cross section in Fig. 7. The moderator assembly is cylindrically symmetric with a 93-cm diameter and a 67-cm axial length. It consists of a 30-cm axially thick, 31 cm diameter cylindrical Fluental moderator, surrounded by a PbF_2 reflector, with a Li_2CO_3 delimiter [25].

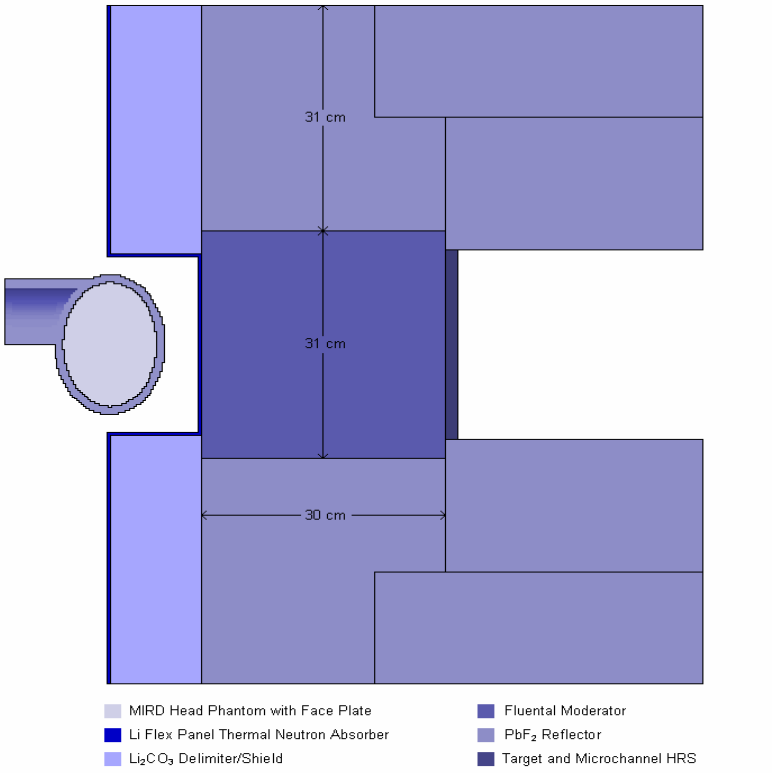

Figure 7. Fluental/PbF_2 moderator assembly design

As a second step we re-evalauated the moderator assembly materials with an expanded set of goals. The goals were to maximize $D_{tumor,6cm}$,maintain T below 30 minutes per fraction for a four fraction treatment plan with a 10 mA proton beam, reduce material costs, and use materials that do not activate to produce a large gamma-ray source activity, or transmute to radiotoxic materials that may pose a problem for decommissioning. We maintained the basic geometry that is shown in Fig. 7, but varied the relative dimensions of the various regions of the moderator assembly as we changed the materials in those regions. We found that a moderator assembly, with MgF_2 as the moderator material and CaF_2 as the reflector and delimiter materials, better satisfied our expanded set moderator assembly design goals.

As a third step we re-evaluated the moderator assembly geometric design with MgF_2 as the moderator material and CaF_2 as the reflector and delimiter materials. The base moderator assembly geometric design is presented in Fig. 7. Modifications to this design were considered with the goal of reducing the moderator assembly size, and hence the cost of its materials and its manufacturing, while maintaining $D_{tumor,6cm}$ acceptably large and T acceptably small. The other important change that was made in the base

moderator assembly design was to modify the details of the shape of the moderator according to the predictions of simple Fermi Age Theory calculations. Using this theory to guide our modifications of the shape, while using MCNP to determine $D_{tumor,6cm}$ and T for the resulting moderator shapes; the moderator shape was modified such that shorter Ts were obtained without a corresponding negative impact on$D_{tumor.6cm}$. The modified shape of the moderator assembly is a cylindrical-truncated cone. Figure 8 shows the configuration of this moderator assembly design [26]. This moderator assembly, 25 MgF2 /25-56 CaF2/CaF2 exhibited a short treatment time, 60 min, with an appropriately large $D_{tumor,6cm}$ (1975 cGy). For this moderator, the accelerator current could be reduced from 10 mA to approximately 5 mA without exceeding the 120 minute limit on treatment time.

The moderator assembly's lateral profile is that of a right circular cylinder. However, it is in fact comprised of a number of objects of revolution: specifically a MgF_2 moderator, a CaF_2 reflector, and a CaF_2 delimiter. The lithium target and the target Heat Removal System (HRS) abut the moderator on its upstream side. The treatment port lies immediately downstream of the moderator and is formed by the hole in the center of the annular delimiter. The dimensions of the components of the moderator assembly are given in Fig. 8.

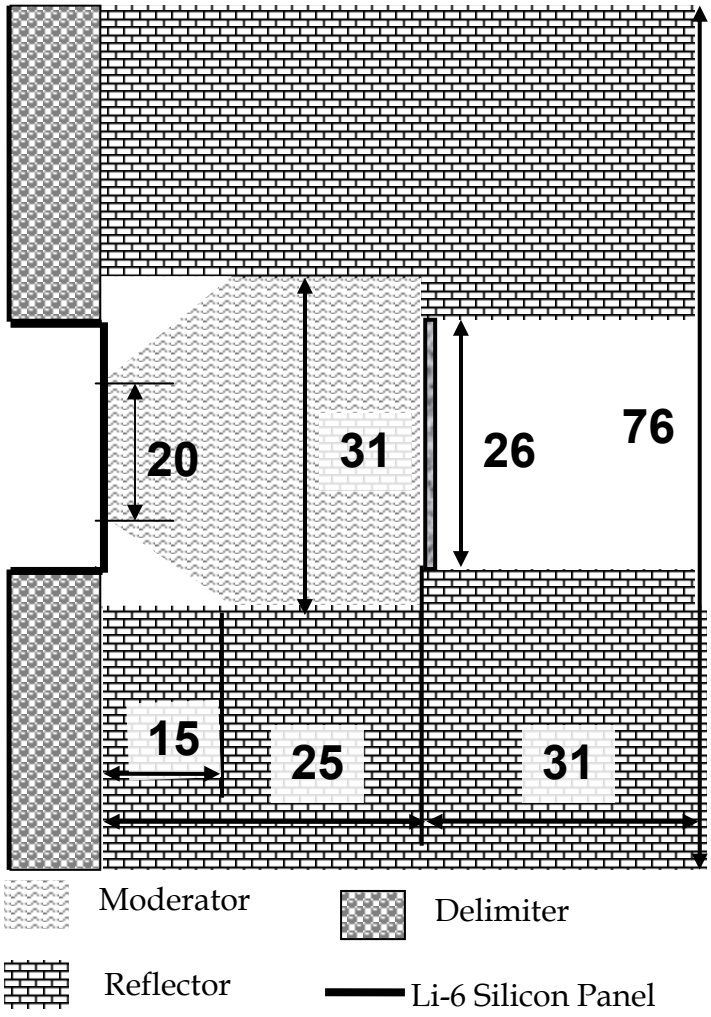

Figure 8. Geometry of the moderator assemblies (dimensions in cm)

The moderator assembly functions as follows. The proton beam enters the moderator assembly through the beam port the right hand side of Fig. 8. Beam protons strike the target causing the emission of neutrons. The neutrons emitted in the target pass through the moderator before irradiating the patient. In passing through the moderator, the average energy of neutrons is reduced to epithermal energies which are appropriate for BNCT. In moderating the neutrons to epithermal energies, the moderator provides some degree of protection to the patient with respect to fast neutron whole body dose. The moderator also shields the patient from gamma rays emitted in the target. Additional shielding is provided by the delimiter.

The intent of the delimiter is that it delimits the neutron field entering the patient. In so doing it shapes the radiation dose distribution within the patient's head and shields the patient's whole body from fast neutrons, epithermal neutrons and gamma rays.

Additionally the downstream surface of the delimiter and the portion of the moderator assembly that forms the treatment port are lined with a thin layer of a lithiated silicon flex panel, which shields the patient form thermal neutrons.

1.1.5 Delimiter Design Using Zubal Phantom

As the fourth step in the moderator assembly redesign, we examined the effectiveness of the delimiter in performing its dual roles of shaping the radiation dose distribution within the head and reducing the patients whole body radiation dose. In addition, the effect of the delimiter on the treatment time was examined. Of the many parameters that may be varied in the design of a delimiter, only two (the axial thickness of the delimiter and the diameter of the treatment port) were considered in our analysis.

1.1.5.1 Patient Phantoms

We used two different phantoms for these studies. For the purposes of calculating the effectiveness of the delimiter in shaping the radiation dose distribution within the patient's head, we used the Zubal phantom. Hereafter such calculations will be referred to simply as Zubal phantom calculations. For the purposes of calculating the effectiveness of the delimiter in reducing the patient's whole body dose we used the MIRD phantom. Hereafter, such calculations will be referred to simply as MIRD phantom calculations. It should be noted that the calculations with the Zubal phantom include the torso and upper extremities of the MIRD phantom. The Zubal and MIRD phantoms are described below.

1.1.5.1.1 Zubal Phantom

The original Zubal phantom is a 3-D model of a head that was created from MRI images of a healthy human male that delineates phantom structures [Zubal et al.(1994)] [27]. In order to calculate the dose to tumor, we inserted a spherical tumor with a 1cm diameter within the phantom at 6cm depth, as measured from the inner surface of the skull along the beam centerline. Also, as described in Evans et al. (2001) [28], the phantom was compressed into an 85×109×120 one-byte array and translated into lattice format for entry into MCNP. Figure 9 shows a transverse cross-section from the head of the Zubal Phantom, for a slice without tumor.

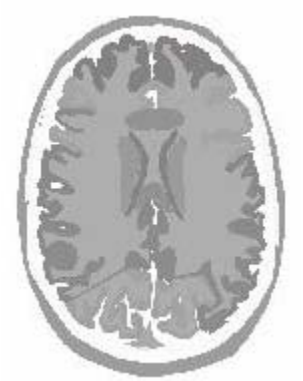

Figure 9. A transverse cross-section from the head of the Zubal Phantom as viewed with ImagJ

1.1.5.1.2 MIRD Phantom

The mathematical patient phantom used in the shielding calculations was the adult male phantom developed by Cristy and Eckerman (1987) [29]. The Cristy/Eckerman phantom represents the human form and its internal organs by using the mathematical equations of standard geometric shapes. It incorporates the major organs used in International Commission on Radiological Protection (ICRP) whole body dose calculations. It was revised in 1996 to include an esophagus and a neck section [30] and these revisions to the phantom were included in our modeling. In this study, the phantom was only used to estimate the absorbed dose to the red bone marrow and to provide an appropriate scatterer for returning neutrons to the head by reflection. Consequently (with the exception of the head) the lungs, skeletal system, and the body remainder were the only three tissue types included in the phantom. The compositions for these three tissues were taken from the Cristy/Eckerman 1987 report.

The phantom represents a male with height 1.74 m and a proportionate mass of 70 kg. Figure 10 is an anterior oblique view of the Cristy/Eckerman phantom. Note that the lungs are included in the skeletal image.

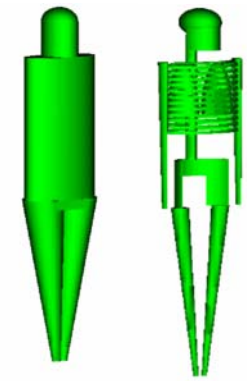

Figure 10. Anterior oblique view of the Cristy/Eckerman phantom and phantom skeleton

In order to calculate the dose along the centerline of the brain in the MIRD phantom we inserted a series of 64 cylindrical detectors, 0.4 cm in diameter and 0.2 cm tall, along the centerline of the brain.

1.1.5.2 Model Geometry

As shown in Fig. 11, for the moderator assembly calculations, the phantom was positioned such that the centerline of the moderator assembly was collinear with the centerline of the head phantom, and such that the top of the head was aligned with the downstream surface of the delimiter. Due to the lattice entry format for our implementation of the Zubal phantom, the details of that phantom are contained within the rectangular parallelepiped that is shown in the figure. For the INS calculation, the phantom was positioned such that the centerline of the circular INS source was collinear with the centerline of the head phantom. The neutrons were directed such that they were perpendicularly incident on the upstream surface of the rectangular parallelepiped (i.e., the top of the patient's skull.)

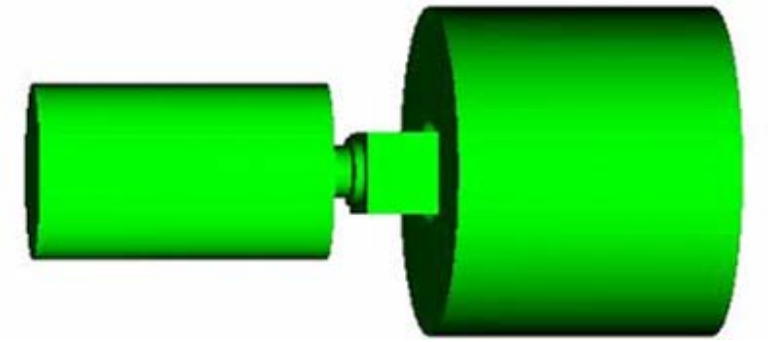

Figure 11. Patient orientation with respect to the moderator assembly

In order to assess the effectiveness of the delimiter in shaping the radiation dose distribution within the patient's head, we defined a new neutron field assessment parameter (NFAP). This new NFAP was developed to evaluate the complex dose distributions resulting from the mixed neutron and gamma ray fields that arise in the head of an individual who is treated for a malignant brain tumor using BNCT. The modified Zubal phantom was used to calculate the absorbed doses of different structures in the brain as well as the tumor dose. The new NFAP is based on absorbed dose distributions for normal structures and tumor, and yields a score that accounts for the competing goals of (1) sparing normal tissues and (2) maximizing tumor dose. It was formulated by modifying a previously defined Objective Function (OF), so that it is appropriate for

BNCT. The resulting BNCT Objective Function (BOF) allows for the inclusion of tissue specific Relative Biological Effectiveness (RBE), and tissue specific dose tolerances and weights.

In BNCT, the absorbed dose to an organ is largely dependent on the concentration of the boron-containing compound within that organ. The concentration of boron in red bone marrow is not well known, but it is believed to be low enough that it can be ignored in calculation of the absorbed dose. For this reason, the red bone marrow absorbed dose, in the absence of boron, is used to assess the degree of patient protection provided by the moderator assembly delimiter. The kerma factors for red bone marrow listed in the International Commission on Radiological Units (ICRU) publication 46 [31] were used in this work for the calculations of absorbed dose to the red bone marrow. The absorbed dose in the red bone marrow, per source neutron was tallied, in MCNP, for the entire bone marrow volume in the MIRD phantom.

1.1.5.3 Results

With a treatment port diameter of 25cm, none of the delimiter thicknesses meet the criteria that HRM remain less than 0.5Sv. With a treatment port diameter of 15cm and a delimiter thickness of 13cm or more HRM is less than 0.5Sv. Of these 3 delimiters, 15cm diameter 13cm thickness (15-13),15cm diameter 15cm thickness (15-15), and 15cm diameter 17cm thickness (15-17), the 15-13 configuration has the highest value of F at w=1 (in fact it has the highest value of F at all 3 values of w(a tissue weighting factor)) and the shortest treatment time. In conclusion, the best delimiter evaluated in this work is one with a 15cm treatment port diameter and a thickness of 13cm (15-13).

1.2. Experimental Studies - Moderator Assembly Experimental Verification

In this section, the verification of our in-air and in-phantom design methods by measurement are described. The fabrication of the moderator assembly was completed by Gupta [32,33]. Improvements to this moderator assembly were made by Doblebower. They are discussed in his Ph.D. Dissertation [34]. The experimental verification was performed at Ohio University in Athens Ohio. The accelerator at this facility is capable of producing approximately 20 microamps of 2.5 MeV protons at the target. The types of verification experiments which were performed included both measurements from a bare

^{7}Li target and measurements in the irradiation port of the moderator assembly. Each of these sets of experiments and their results is discussed in the following sections.

1.2.1 Bare Target Measurements

The bare target measurements were made in order to confirm the source term used in the moderator assembly neutronic calculations. These measurements were made in front of the target and beam monitor without the moderator assembly in place. The neutron beam monitor was an air ionization chamber whose function is to provide an indication of the neutron production rate from the target in order to verify the integrity of the lithium target.

1.2.1.1. Proton Recoil Measurements

A Proton Recoil Proportional Counter (PRPC) was used to measure the neutron spectrum from the target. It is an appropriate detector, because most of the neutron flux spectrum from the target occurs for neutron energies above the threshold of the detector (about two hundred keV) [35,36]. The PRPC was placed 8 feet from the target along the beam line. The measurement was performed three times at this location (designated run 1, run 2, and run 3) to show the precision of the experiment. The setup for this experiment is shown graphically in Figure 12.

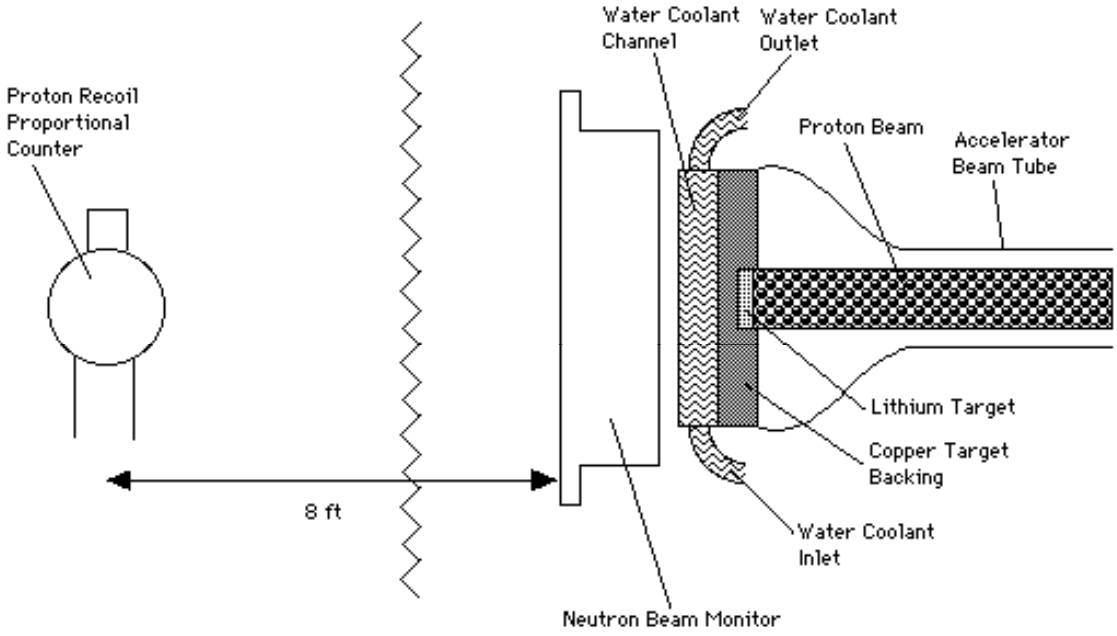

Figure 12: Experimental setup for proton recoil measurements

A histogram of the calculated and measured neutron fluence per unit lethargy per coulomb of protons on target vs. neutron energy is shown in Figure 13. It can be seen from Figure 13 that the shape and magnitude of the calculated and measured neutron spectra agree well. Both the calculated and measured neutron spectra peak at approximately 500 keV. The magnitude of the calculated and measured spectra differs by approximately 15%. This discrepancy could be due to positioning errors with the PRPC and modeling deficiencies, such as the angular dependency of the neutron source at small forward angles.

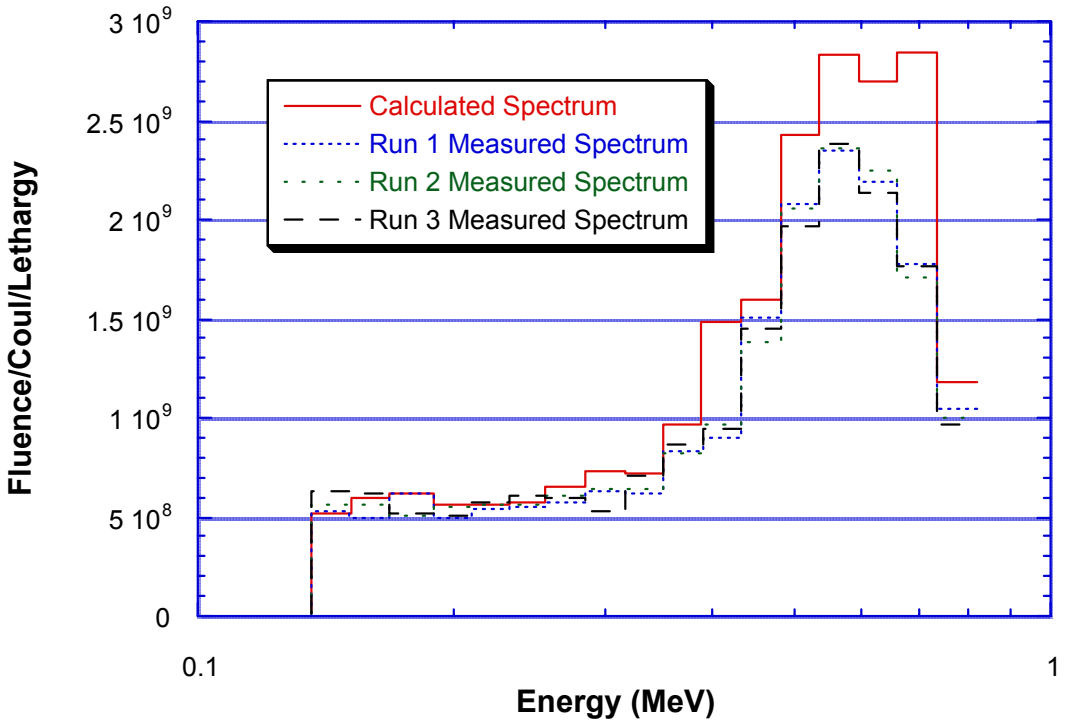

Figure 13: Calculated and measured neutron spectra from the bare target assembly

1.2.1.2. Paired Ion Chamber Measurements

The purpose of the work which is reported in this section was to confirm, by measurement, neutron and gamma-ray absorbed dose rates calculated with MCNP in the mixed field immediately downstream of the target assembly for an ABNS for BNCT. The measurements were made using the paired Ion Chamber (IC) technique.

The experimental equipment used to perform the measurements consisted of one set of paired ionization chambers, a gas flow system, a high voltage supply, and an electrometer. The center of each detector was positioned on the beamline axis at a distance of 2.4 cm from the downstream face of the neutron beam monitoring device (see Figure 14).

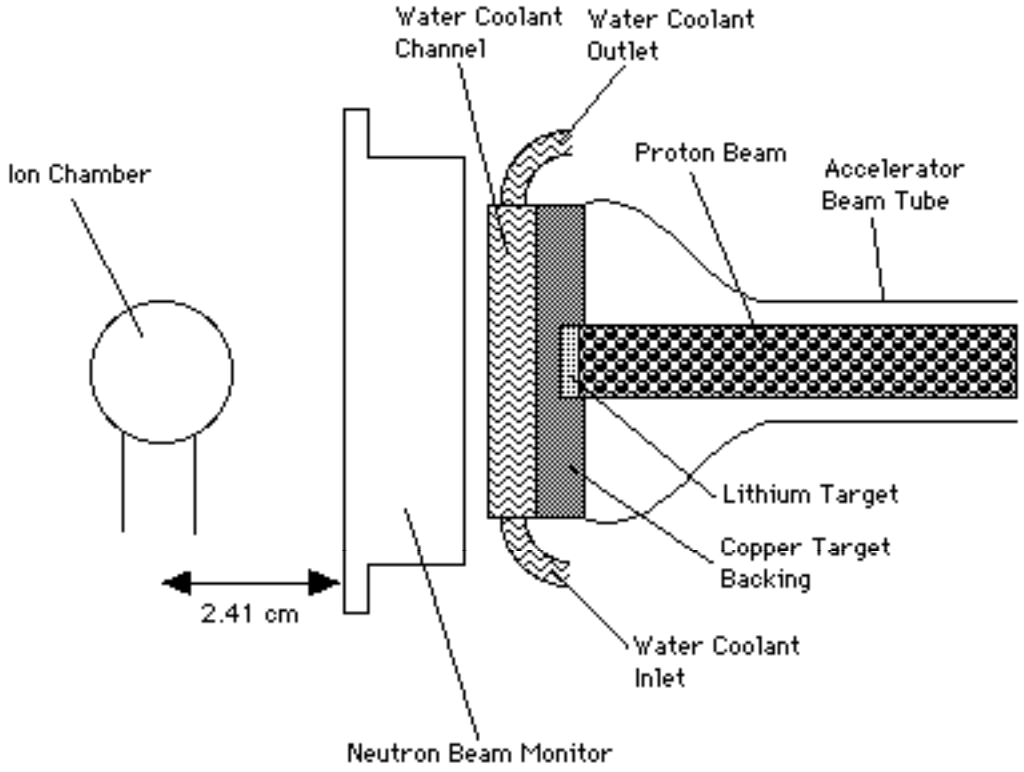

Figure 14: Experimental setup for paired ion chamber measurements

The paired IC's, which were used, were supplied by Far West Technology (FWT). The pair consisted of a TE-walled and Mg-walled ion chamber. The IC's were FWT's model IC-17 (TE) and IC-17M (Mg) with sensitive volumes of approximately 1 cc and 2 cc, respectively. The mass wall thickness of the 1 cc TE IC is 569 mg/cm^2 and 544 mg/cm^2 for the Mg IC. The wall thickness of the IC's provide charged particle equilibrium for photons with energies up to the energies of ^{60}Co gamma-rays. Neutron charged particle equilibrium was provided up to 20 MeV.

The absorbed dose components were determined using the measured responses of the ionization chambers, and the appropriate chamber sensitivities. The responses of the

ion chambers were corrected for temperature, pressure, and leakage, and were normalized to the amount of charge deposited on the target during the time interval for which the response was measured, q_{targ}. The neutron and gamma absorbed dose per unit charge on target, hereafter called the specific absorbed dose and denoted d_N and d_G respectively, along with the corresponding values calculated with MCNP, 2.4 cm downstream of the target assembly are shown in Table 2.

	MCNP	Measured	Difference
d_N (cGy/q_{targ})	4120 ± 0.3 %	3700 ± 14 %	11 %
d_G (cGy/q_{targ})	120 ± 6 %	140 ± 12 %	-14 %

Table 2: Target Assembly Results Comparison

The neutron specific absorbed dose was measured to be 3700 cGy/C. The measured neutron specific absorbed dose is within one standard deviation of the neutron specific absorbed dose of 4120 cGy/C predicted by MCNP calculations. The measured gamma specific absorbed dose was 140 cGy/C which differs from the gamma specific absorbed dose of 120 cGy/C predicted by MCNP by less than one standard deviation of the combined uncertainties in the measurement and the calculation. These measurements pointed out the importance of including gamma ray production by the Li-7(p,p') reaction in our calculations. According to our calculations, this reaction contributes 93% of the measured gamma ray dose for thick Li-7 targets.

1.2.2. Moderator Assembly Measurements

Measurements with the moderator assembly were performed in order to confirm calculational techniques. These measurements were made inside or immediately outside of the moderator assembly's treatment port where patient irradiations would take place. The measurements with the moderator assembly include sets of both in-air and in-phantom measurements. Each of these measurements is discussed in the following sections.

1.2.2.1 In-Air Measurements

In-air measurements were performed to confirm calculations of the neutron and gamma fields in the treatment port of the moderator assembly. The in-air measurements consisted of two sets of experiments. The first set of experiments used a PRPC in combination with a Boron Shell Detector (BSD) to measure the neutron spectrum. The second set of experiments used the paired ion chamber technique to measure the neutron and gamma-ray absorbed dose rates. Each of these measurements is discussed in the following sections.

Neutron Spectrum Measurements

The neutron spectrum measurements were performed to confirm the neutron spectrum calculations in-air beyond the moderator assembly. The setup for this measurement is shown graphically in Figure 15. These measurements were made immediately outside of the treatment port of the moderator assembly. The measurements of the neutron spectrum were made using both the PRPC and the BSD.

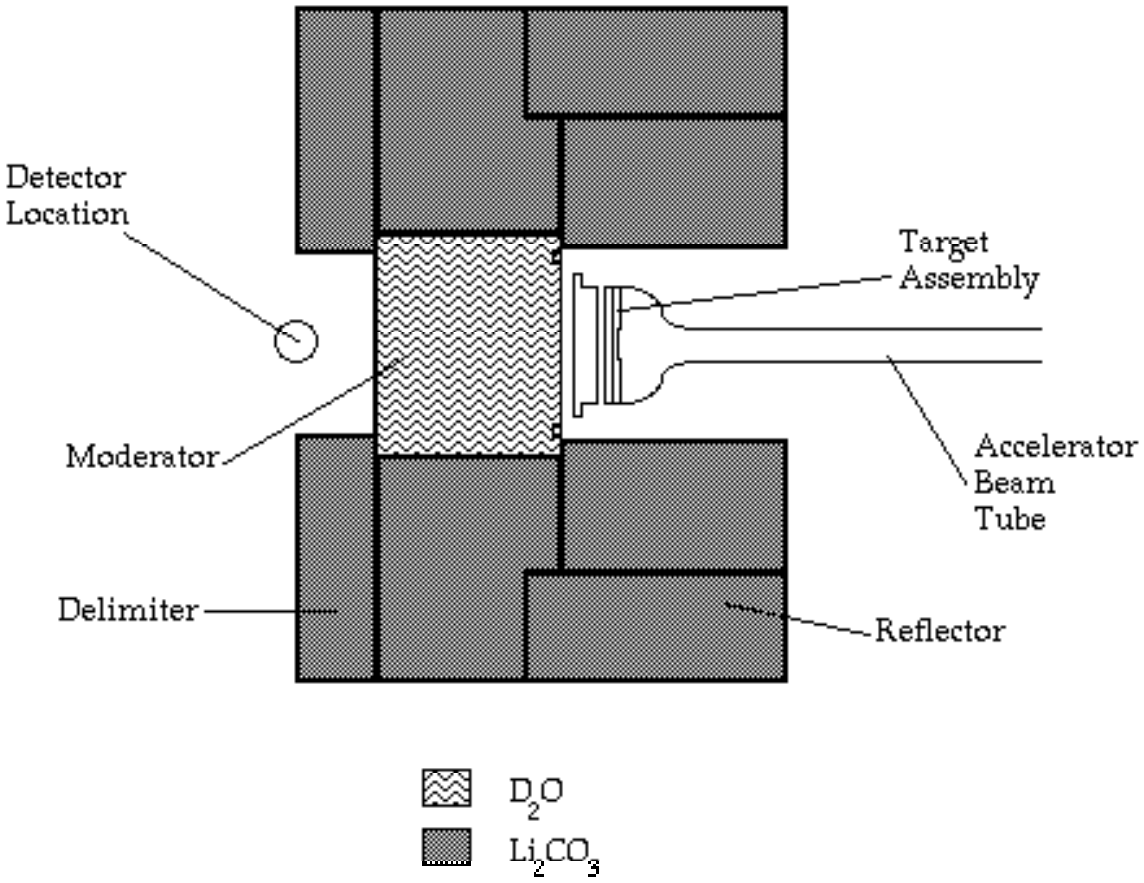

Figure 15: Experimental setup for in-air measurements

A graph of both the calculated and measured neutron fluence per unit lethargy per coulomb of protons on the target vs. neutron energy is shown in Figure 16. This graph shows good agreement between the calculated and measured neutron flux spectra. A discontinuity is observed in the measured flux spectrum at approximately 30 keV. This discontinuity occurs at the energy limits of the PRPC and the BSD as the two measurement techniques produce slightly different results at this energy. It is also noted that the PRPC measurement agrees well with the calculations especially at higher energies, while the BSD measures slightly higher than the calculated spectrum at higher energies and slightly lower than the calculated spectrum at lower energies. The small discrepancies between the calculated and measured neutron spectra, at the lower energy range of the PRPC, could be due to uncertainties in the gas multiplication of the PRPC, when operated at higher voltages. The discrepancies between the calculated and measured neutron spectra, over the energy range covered by the BSD, could be due to an uncertainty in the ^{10}B loadings in the shells of the BSD.

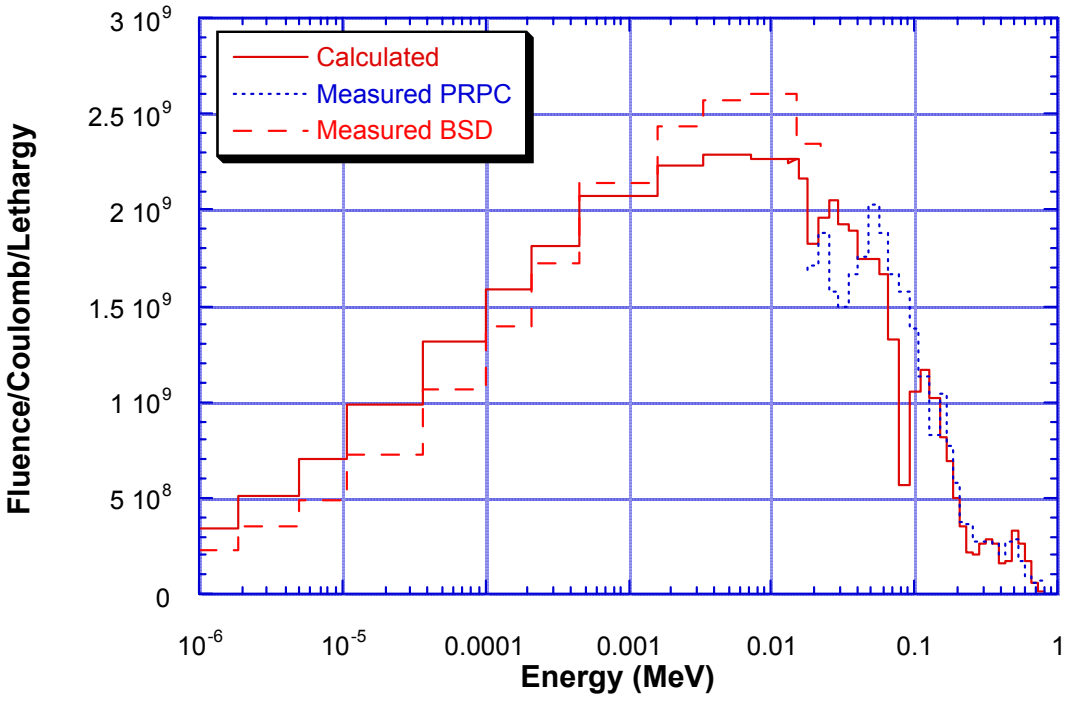

Figure 16: Calculated and measured neutron spectra from the moderator assembly

Paired Ion Chamber Measurements

Measurements in the moderator assembly treatment port using the paired ion chamber technique were performed. Large ion chambers were used, because for the small ion chambers, the charge collected from the ion chambers was small compared to the charge collected due to leakage currents. The results of the measurements are presented in Table 3. They show that there is good agreement between the calculated and the measured neutron dose, but that the calculated gamma ray dose is smaller than the measured gamma ray dose by approximately 60%. This indicates that there is a component of the gamma ray dose, which was not included in our calculational model. We did not put much effort into identifying the source of the additional gamma-ray dose, because, based on our subsequent design work, we decided to change the moderator assembly materials.

	Calculated	Measured	Difference
d_N (cGy/q_{targ})	2.97±7%	3.1±14%	-4%
d_G (cGy/q_{targ})	1.09±4%	3.05±1%	-64%

Table 3. Calculated and Measured specific absorbed doses downstream of the target and moderator assemblies.

1.2.2.2. In-Phantom Measurements

In-phantom measurements were performed to confirm calculations of the neutron flux profiles in various phantoms. The in-phantom measurements consisted of two sets of experiments. The first set of experiments was performed with a small ^{3}He neutron detector and a box shaped water phantom. The second set of experiments was performed with the same ^{3}He detector and an acrylic ellipsoidal head phantom. Each of these measurements and their results is discussed below.

Water Phantom

The water phantom measurements were performed to confirm neutronic calculations of the neutron field assessment parameters T and D_{Tumor} which are based on

the absorbed dose profiles in the phantom. The setup for these measurements is shown graphically in Figure 16. The measurements were performed in a water phantom with its upstream face located 3/8 inch outside the treatment port of the moderator assembly and with its centerline colinear with the moderator assembly's centerline. This location was chosen because it represents a possible location of a human head during therapy.

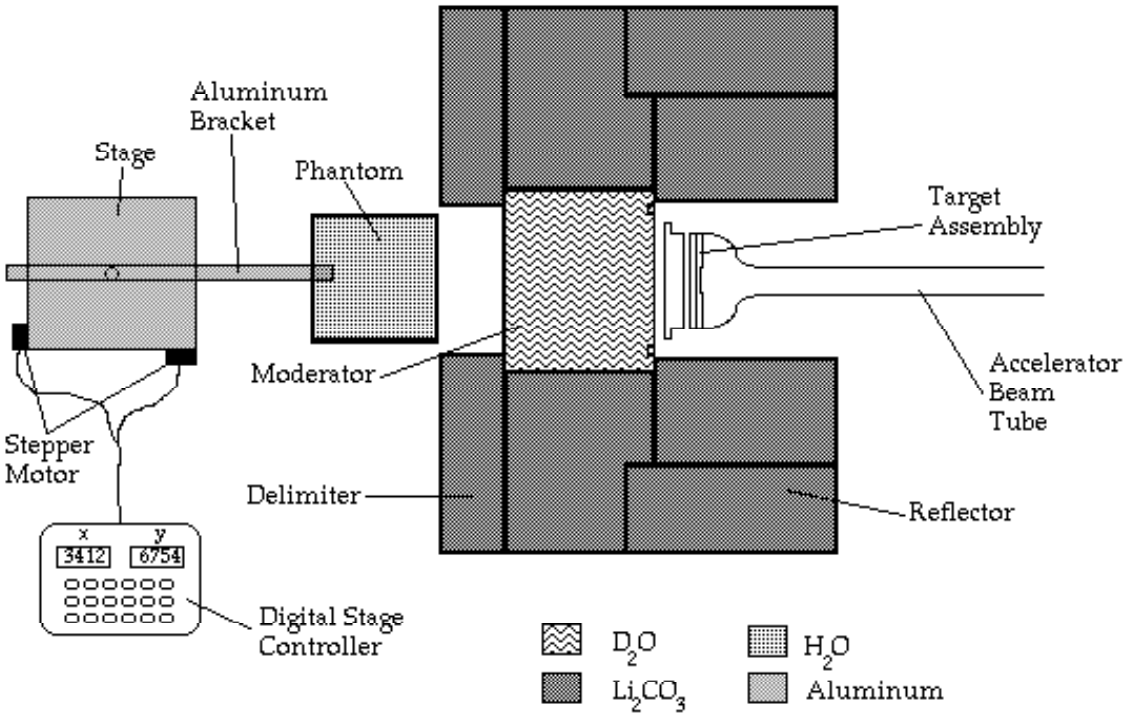

Figure 17: Experimental setup for in-phantom measurements

The in-phantom measurements were performed by scanning the ^3He probe through the water phantom. Two types of scans were performed. The first type of scans performed were "axial" scans along the centerline of the phantom, parallel to the beam line. The second type of scans performed were "horizontal" scans, perpendicular to the axial scans at the axial location of maximum detector count rate from the axial scan. Several points along each scan were repeated to determine the precision of the measurements and the error in the measurement associated with the positioning of the detector.

Graphs of the calculated and measured 2200 m/s fluence per coulomb of protons on target are shown in Figures 18 and 19. These graphs show good agreement between the calculated and measured thermal flux. The average difference between the calculated and measured data is 7.5 and 1.6 % for the axial and horizontal scans, respectively. The small discrepancies between the calculated and measured thermal neutron flux could be due to alignment errors in the moderator assembly with the beam line.

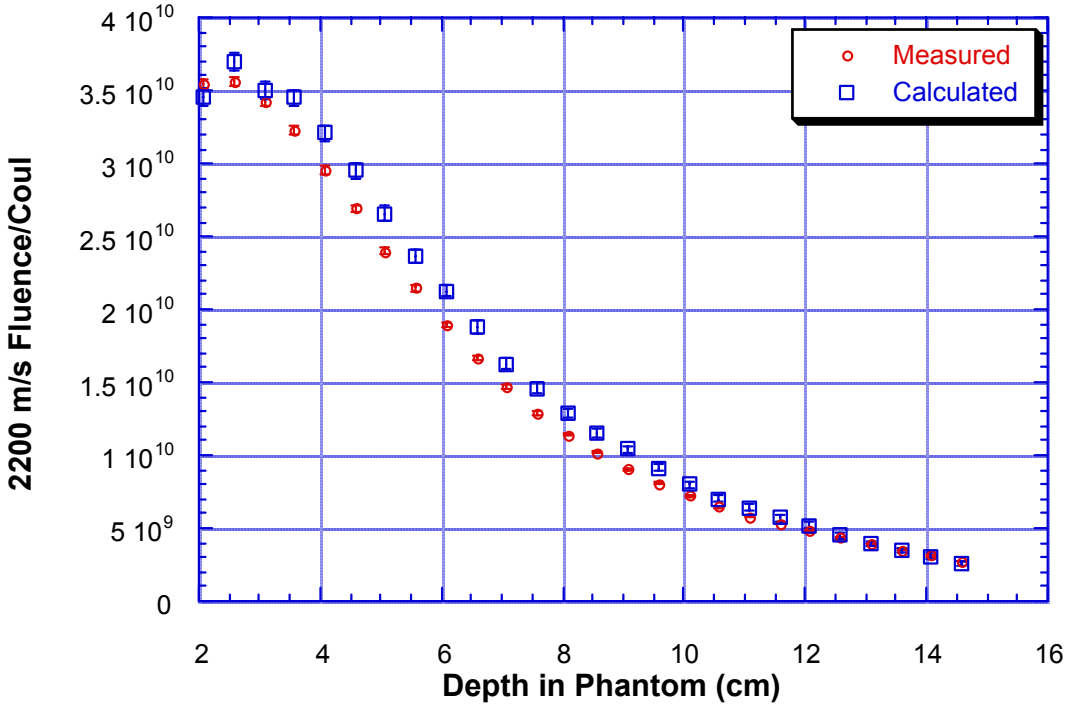

Figure 18: Calculated and measured 2200 m/s neutron fluence per coulomb for the axial scan in phantom

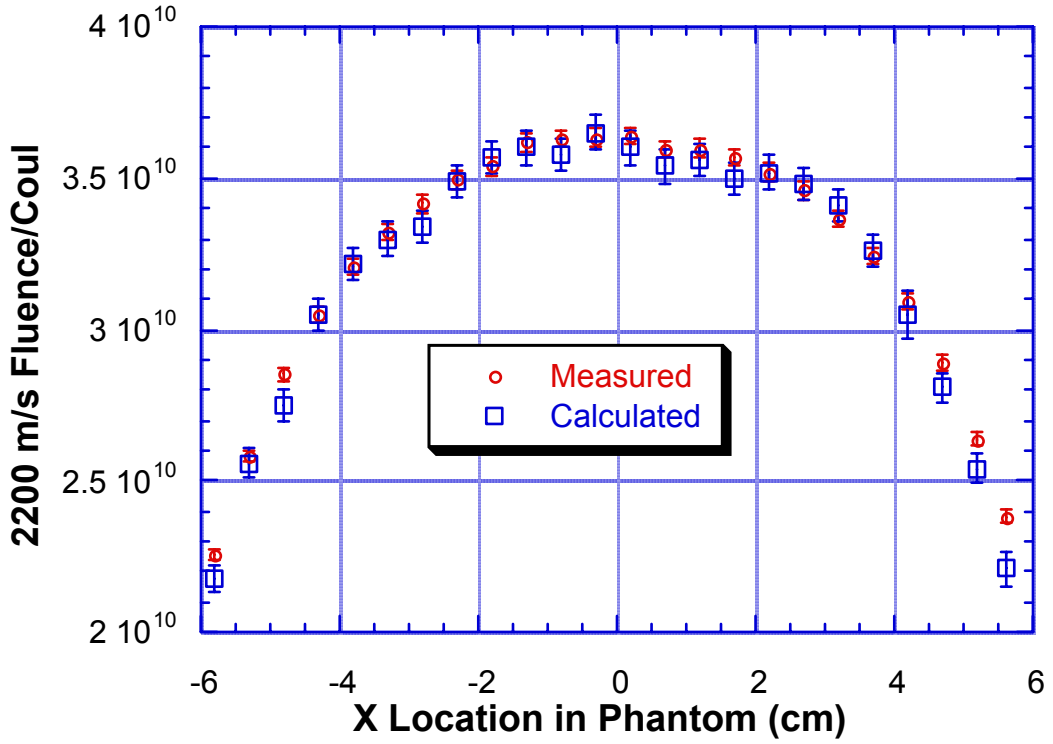

Figure 19: Calculated and measured 2200 m/s neutron fluence per coulomb for the horizontal scan in phantom

Acrylic Phantom

The acrylic phantom is based on the brain of the adult male MIRD phantom [29]. It is an ellipsoid with dimensions of 13.2, 17.2, and 9.5 cm for the x, y, and z axes, respectively. The density of the acrylic was measured to be 1.17 g/cc. For the experimental measurements, this phantom was located within the patient treatment port with its Z (9.5 cm long) axis collinear with the centerline of the moderator assembly, so as to simulate irradiation from the superior aspect. The phantom was inserted into the treatment port deeply enough so that the center of the ellipsoid was exactly in the plane of the front face of the moderator assembly.

For the measurements in the acrylic phantom, the ^{3}He detector was inserted into a hole drilled along the Z axis of the phantom, which was co-linear with the central axis of the moderator assembly. The detector was fitted with an acrylic shroud so that it could be inserted into this hole, without producing large air gaps between the probe and the phantom. The portion of the hole not filled with the detector was back-filled with acrylic

dowels again to remove any air gaps in the phantom. This arrangement is shown in Figure 20. The detector count rate was measured at locations along the axis of the phantom ranging in depth from 4.2 to 11.2 cm in 1 cm increments. The measurements were repeated at all of the detector locations to determine the precision of the measurements.

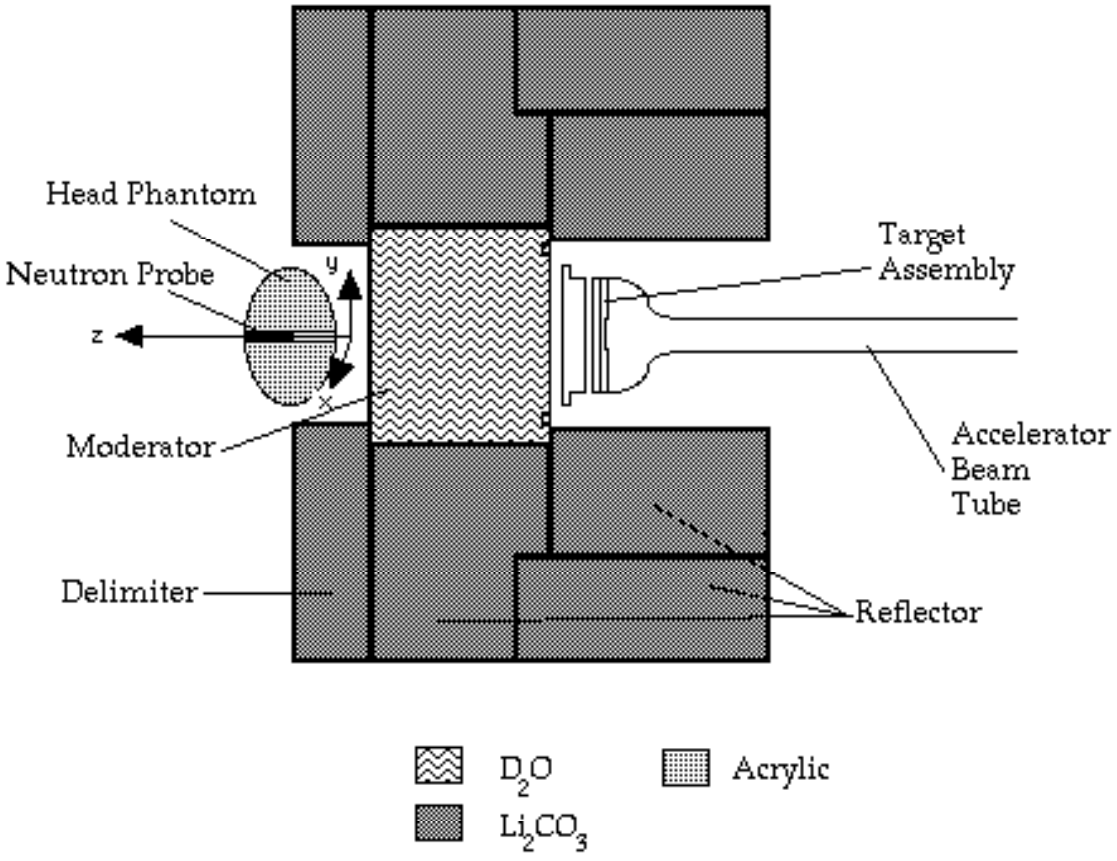

Figure 20: Experimental Setup for the flux measurements in an Acrylic Phantom

The results of the measurements were compared to calculations performed with MCNP and are shown in Figure 21. The calculations have a maximum difference of 24 % and an average difference of 7 % when compared to the measurements in the acrylic phantom.

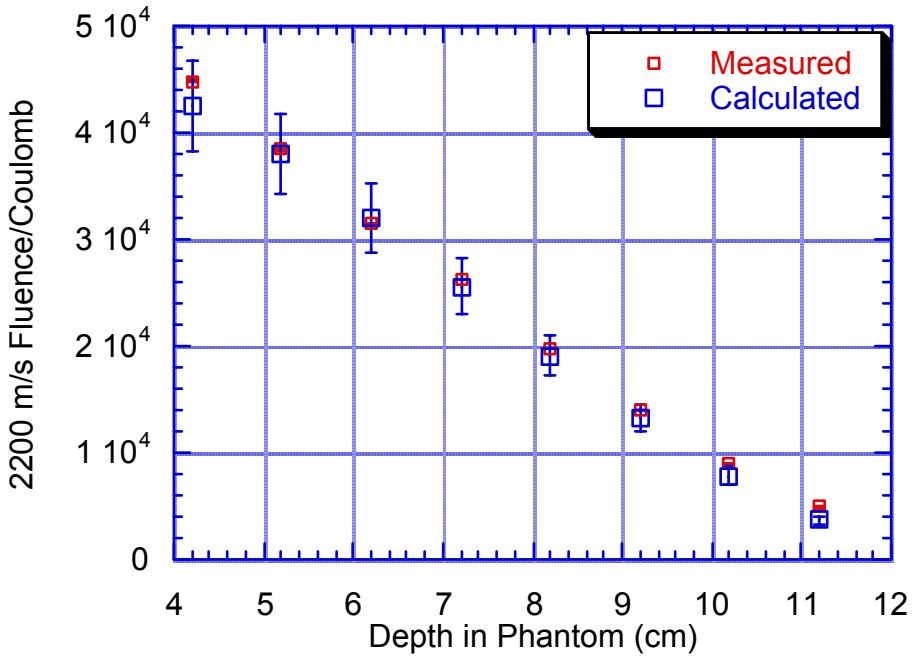

Figure 21: 2200 m/s fluence per coulomb vs. depth (z) in the acrylic phantom along the central axis of the moderator assembly

2. THERMAL-HYDRAULICS AND TARGET ASSEMBLY DESIGN

2.1 Overview

Researchers at OSU, MIT, and LBNL have adopted three different approaches to the challenging problem of cooling the lithium target of the ABNS for BNCT. The problem is challenging, because large heat fluxes must be dissipated (on the order of 2MW/m^2, for the OSU ABNS operating at a beam current of 20 mA), while maintaining the lithium below its melting temperature of 180 C. At OSU, we spent the majority of our time studying the suitability of heat pipes, for the target heat removal system (HRS). Our analysis of heat pipes for the ABNS HRS progressed methodically through a design phase (which included model development, due to the unique geometric configuration of the ABNS HRS heat pipe) to construction and testing. The testing has been at low powers, due to limitations in producing large heat fluxes over extended areas using electric heaters. However, the low power testing showed that our calculations are consistent with our measurements. This provides confidence that the heat pipe, which we have developed, can operate at the high heat fluxes, which will be produced during the

operation of the ABNS. Further testing of the HRS, would require an accelerator source. Having confirmed our modeling of an ABNS HRS heat pipe design by testing in the lab, we proceeded to examine the competing technologies, which have been developed at MIT (submerged jet) and are being developed at LBNL (microchannel).

Our examination of the submerged jet and microchannel technologies led us to the conclusion that the microchannel HRS should be pursued further. The microchannel HRS offers some advantages over the heat-pipe HRS. First of all, it has already been tested by LBNL, for a size that is appropriate for BNCT, and was found to perform adequately. To ignore the results of the researchers at LBNL would be unscientific and unwise.

Secondly, unlike the heat pipe HRS, which is an integral unit and must be tested as a whole, the microchannel HRS has a repeating structure. It can be tested by examining the heat removal capability of the repeating structure, apart from the microchannel HRS as a whole. This feature is particularly advantageous for testing. Whereas to test the heat pipe HRS, a power of 50 kW must be deposited in the target HRS, for a microchannel HRS consisting of 25 repeating microchannel structures, only $1/25^{th}$ of that power, or 2kW, must be deposited in the repeating structure of the microchannel , in order to test it. We were able to test our heat pipe HRS to a heat flux of only about 0.016 MW/m^2, because of this problem. On the other hand, we tested the repeating structure of the microchannel, which we fabricated, using electric heaters in our lab to a heat flux of approximately 4 MW/m^2.

Thirdly, the microchannel HRS is neutronically advantageous relative to the heat pipe HRS, for the following reasons: 1) The volume of the heat pipe greatly exceeds the volume of the microchannel HRS. 2) The axial dimensions of the microchannel HRS are much smaller than the axial dimensions of the heat pipe HRS. 3) The heat pipe HRS is larger in transverse dimensions, and includes a region of void. 4) The heat pipe HRS requires large quantities of D_2O as a secondary heat sink. In contrast, the microchannel HRS is cooled by a small volume of flowing light water.

Because the microchannel HRS offers some advantages over the heat-pipe HRS, we decided to further examine the microchannel HRS. We copied the LBNL design of a microchannel HRS. A section of the microchannel HRS was fabricated. This microchannel HRS was tested to determine the pressure drop in the channel as a function of mass flow rate through the channel. This testing confirmed the pressure drop versus

mass flow rate data reported by LBNL. Besides verifying the measurements at LBNL, this work demonstrated that microchannels can be manufactured by Electric Discharge Machining (EDM) in Columbus, Ohio with the requisite length of 25 cm, and a smoothness which is adequate and consistent with the smoothness of the manufacturing of the channels at LBNL. Since the performance of the microchannels has been shown to be adequate, in terms of pressure drop versus mass flow rate, we proceeded to test the heat removal capabilities of the microchannel structure.

As discussed above, our heat pipe HRS research has proceeded systematically through a design phase to construction and testing. The testing has been at low powers, due to limitations in producing large heat fluxes over extended areas using electric heaters. Further testing, will require an accelerator source. Since this testing is expensive, and because the microchannel HRS is neutronically advantageous, we view our heat pipe HRS as an alternate technology, which can be tested at high powers, using an accelerator, if for some reason the microchannel HRS should prove to be inadequate.

The remainder of this section describes our development of the microchannel heat removal system in more detail and experimental testing of the microchannel technology.

2.2 Calculational Studies of Microchannel HRS

A computer model of the target and the target HRS was built using a certified thermal-hydraulic code to confirm the experimental results and predict the response of the HRS for different operational regimes. FLUENT CFD (Computational Fluid Dynamics) was chosen as the software package for this task, because of its capabilities and friendly interface with the user. .

2.2.1 Microchannel HRS design and geometry

The Li target is 1 mm thick, and the heat that has to be removed is approximately 25 kW for a 10 mA beam current of protons with 2.5 MeV energy.

The microchannel HRS is a 25 x 25 cm rectangular array of 15 sets of 6 microchannels (Fig.22). Each set of microchannels has a length of 25 cm and a width of 1.76 cm. The lithium target covers entirely the top of the HRS array and the beam is assumed to be circular, azimuthally symmetric with a diameter of 25 cm, and centered on the HRS array.

There are a number of processes to manufacture a microchannel. Examples are mechanical machining, laser machining, or electro-chemical machining. The set of microchannels built for this experimental setup was manufactured using electric discharge machining (EDM). This same process will be used to manufacture the microchannel HRS array. Figure 23 presents the geometry for a single set of six microchannels in the HRS microchannel array (all dimensions are in mm). The set of microchannels which were used for the experiment is almost identical in geometry, the only difference being in the thickness of the aluminum at the top of the microchannels (22 mm for the experiment instead of 2 mm as shown in Fig. 23).

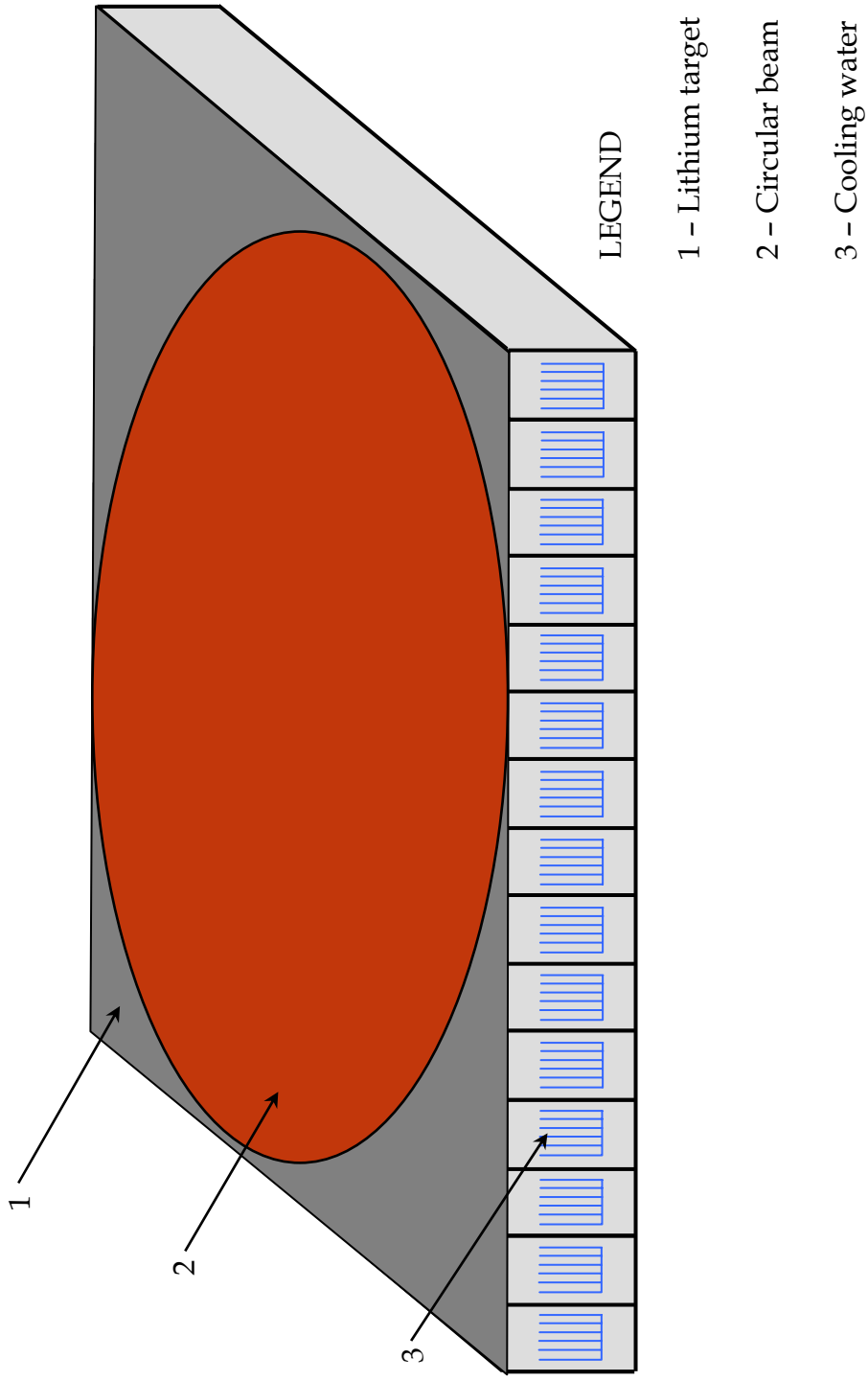

Our design of a microchannel HRS slightly is different than the Lawrence Berkeley National Laboratory (LBL) Design for a heat removal system. We are using 15 identical sets of microchannels to build a 25x25 cm array, and we can say that each set of 6 microchannels is a main unit in the entity represented by the HRS.

In the LBL design, for all but two of the sets of six microchannels, the distance from the water flow path to the lateral surface of the repeated unit is not 2.26 mm (as in Fig. 23) but is 1 mm. The distance of 1 mm to the lateral surface of the repeated unit is modified to be 2.26 mm for the outboard lateral surface of the first and the last sets of microchannels that form the LBL heat removal system design.

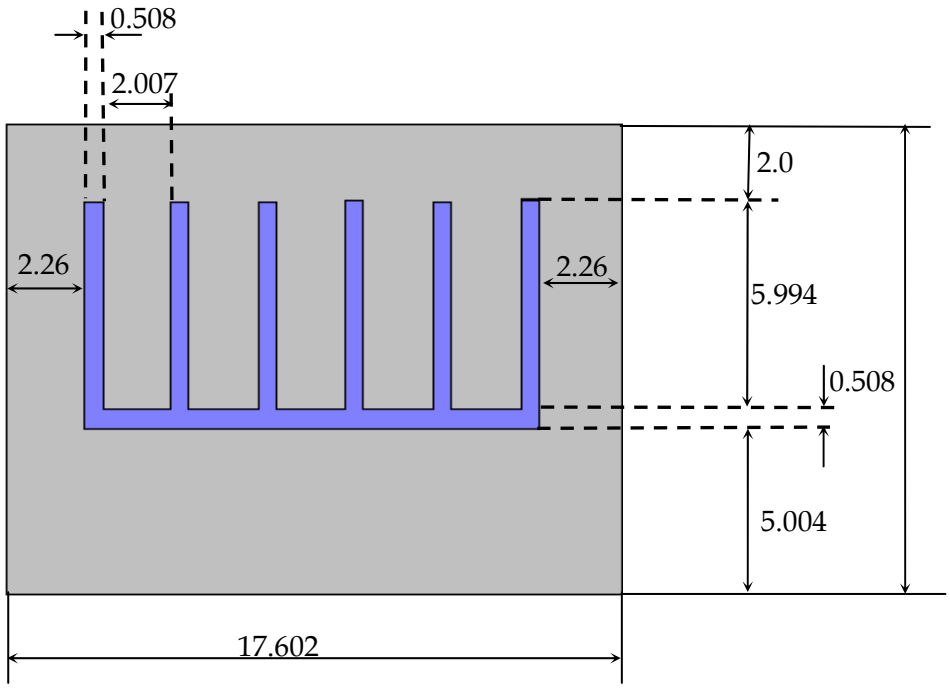

Fig. 23 One set of microchannels in the Microchannel-Based HRS for the ABNS target

Although we've used aluminum to manufacture the experimental set of six microchannels (hereafter called the microchannel test section), this is not the material that will be used to manufacture the HRS. The problem with using aluminum in the HRS design is that it is not compatible with lithium. This fact was understood only after the microchannel test section had been manufactured. A new and compatible material was chosen for the HRS, with excellent thermal conductivity and good structural strength.

This material is Glidcop [37], a dispersion strengthened copper, which has found various applications in accelerator designs within the past decade. Glidcop has thermal and electrical conductivities similar to OFE copper (Oxygen Free). Unlike OFE,

however, Glidcop has yield and ultimate strengths equivalent to those of mild-carbon steel, making it a good structural material. It can be fabricated into shapes and assemblies using processes that are very similar to those used with OFE copper.

There are a number of Glidcop alloys. The Glidcop alloy which was chosen for the target HRS is Glidcop Al-60. This alloy contains 0.3% aluminum oxide and has an excellent thermal conductivity of 365 ($W \cdot m^{-1} \cdot K^{-1}$). This thermal conductivity is better than that for aluminum (with a thermal conductivity of 240 ($W \cdot m^{-1} \cdot K^{-1}$))

Because of the complexity of the geometry of the microchannel HRS array (15 sets of microchannels in parallel),the analysis of the microchannel HRS was simplified to the consideration of a single set of six microchannels. The most limiting case was considered in the calculations (both the analytical model which was developed using the experimental results and the computational model).

Because the distribution of the beam flux was assumed to be Gaussian, with its center at the center of the microchannel HRS, with a peak to average power ratio of 3.1, the central set of microchannels represents the most limiting case. This set of microchannels has to transfer a thermal load that is bigger than the thermal loads that are imposed upon the other microchannels. The thermal load is biggest for the central set in two senses. First of all, the peak heat flux is a maximum for the central microchannel set. Secondly, the average heat flux is largest for the central microchannel set, because the chord length across the beam is greatest for this microchannel set (the chord length across the beam is exactly the beam diameter, which equals the length of the microchannel).

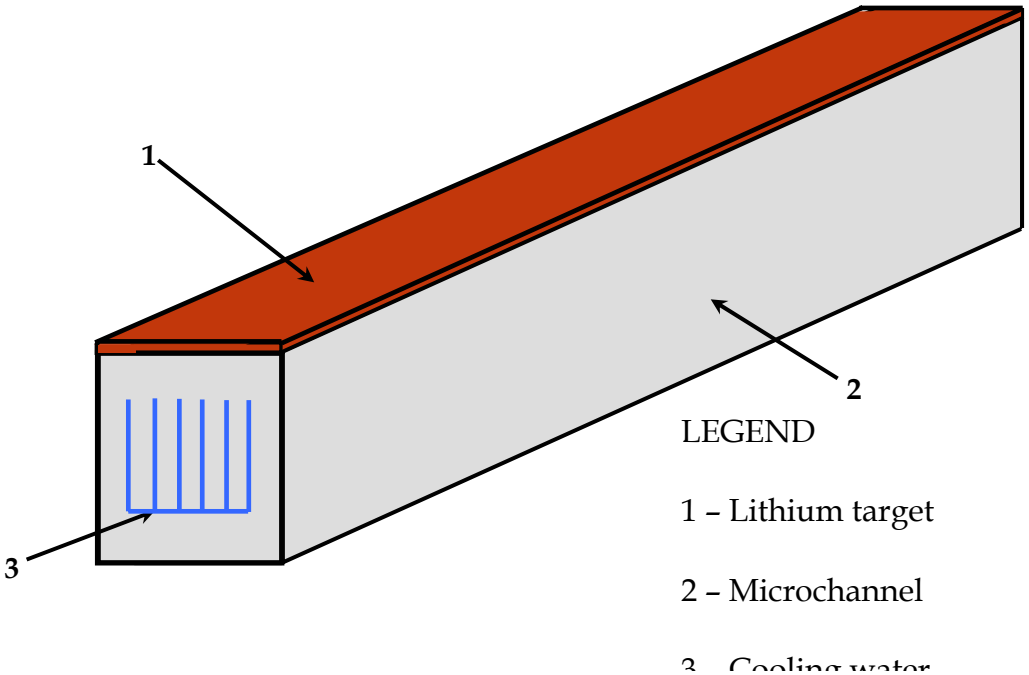

Fig. 24 HRS Central Set of Microchannels

As stated previously, there are 15 sets of microchannels in the HRS array. These 15 sets of microchannels have to evacuate the power which is deposited in the lithium target (approximately 25 *kW*). For a Gaussian beam power distribution with a beam peak to average power ratio of 3.1, the power which is incident upon the central microchannel set was calculated to be 3.5 *kW*. This power is two times the power which is incident upon a set on average.

The results for the spatial temperature distribution are given by Fig. 25.

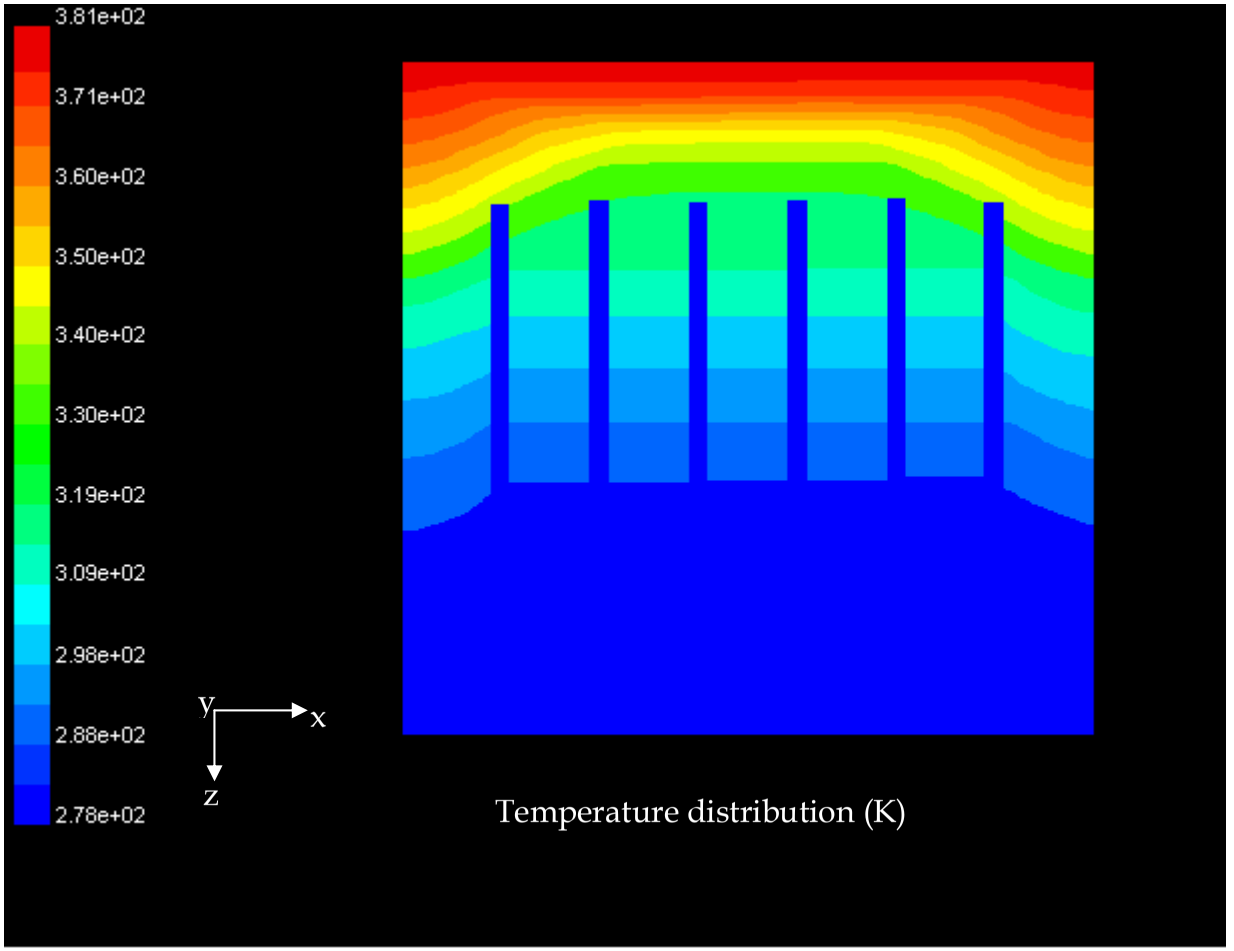

Fig. 25 The spatial temperature distribution in lithium, Glidcop and water

It can be observed that the maximum temperature in the lithium target is 108 ^{0}C which represents a temperature lower than the lithium melting point (180 ^{0}C) by 72 ^{0}C. The temperature of the Glidcop top surface ($T_{top,Glidcop}$) is approximately 79 ^{0}C and the bulk temperature is $7^{0}C$.

It should be noted that for the central microchannel set average power (P_{ave} = 3.5 kW) only the uniform heat flux q''_{ave} was used, instead of a Gaussian beam power distribution with a beam peak to average power of 3.1.

The model predicts the hydraulic parameters obtained in the experiment and although the heat transfer coefficient is smaller, its value is enough to assure the cooling of the lithium target.

2.3 Experimental Studies of Microchannel HRS

The need for a complete thermal and hydraulic experiment came from the fact that there are no conventional transport theories in the literature that can fully explain the phenomena in microscale flow and heat transfer. Also, the smoothness of the microchannel surface was unknown to us.

2.3.1 Microchannel Pressure Drop Experiment

A prototype HRS consisting of six microchannels, including the critical channel, of the full HRS was fabricated. This was incorporated into a closed loop system and the pressure drop in the microchannels was measured. The experimental setup is shown in Figure 26. The microchannel HRS was fabricated from an aluminum block using a wire EDM method. The microchannels are shown in Figure 27. The width of each channel is 0.02" and they are 10 inches long. Experiments were performed that measured pressure drop vs. coolant water flow velocity. The results of the experiment are shown in Figure 28. The measurements were repeated 3 times to show the precision of the experiments and are designated group 1, group 2, and group 3.

Figure 26. Microchannel pressure drop experimental setup.

Figure 27. Close-up view of the microchannels cut in the target block.

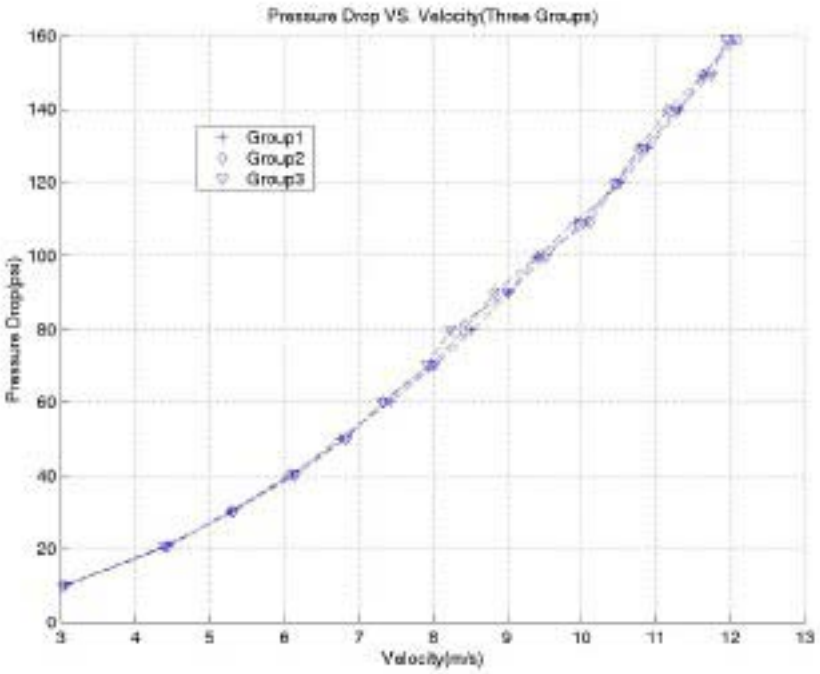

Figure 28. Microchannel pressure drop experimental results.

2.3.2 Microchannel Heat Transfer Coefficient Experiments

The experimental setup consisted of a single set of the 15 microchannel sets that comprise the microchannel array manufactured from aluminum. The beam heating was simulated using 7 electrical heaters in copper blocks as shown in Fig 29.

Twenty-eight experiments were run and the global heat transfer coefficient (h) was determined to be 40,000 W m^{-2} C^{-1}

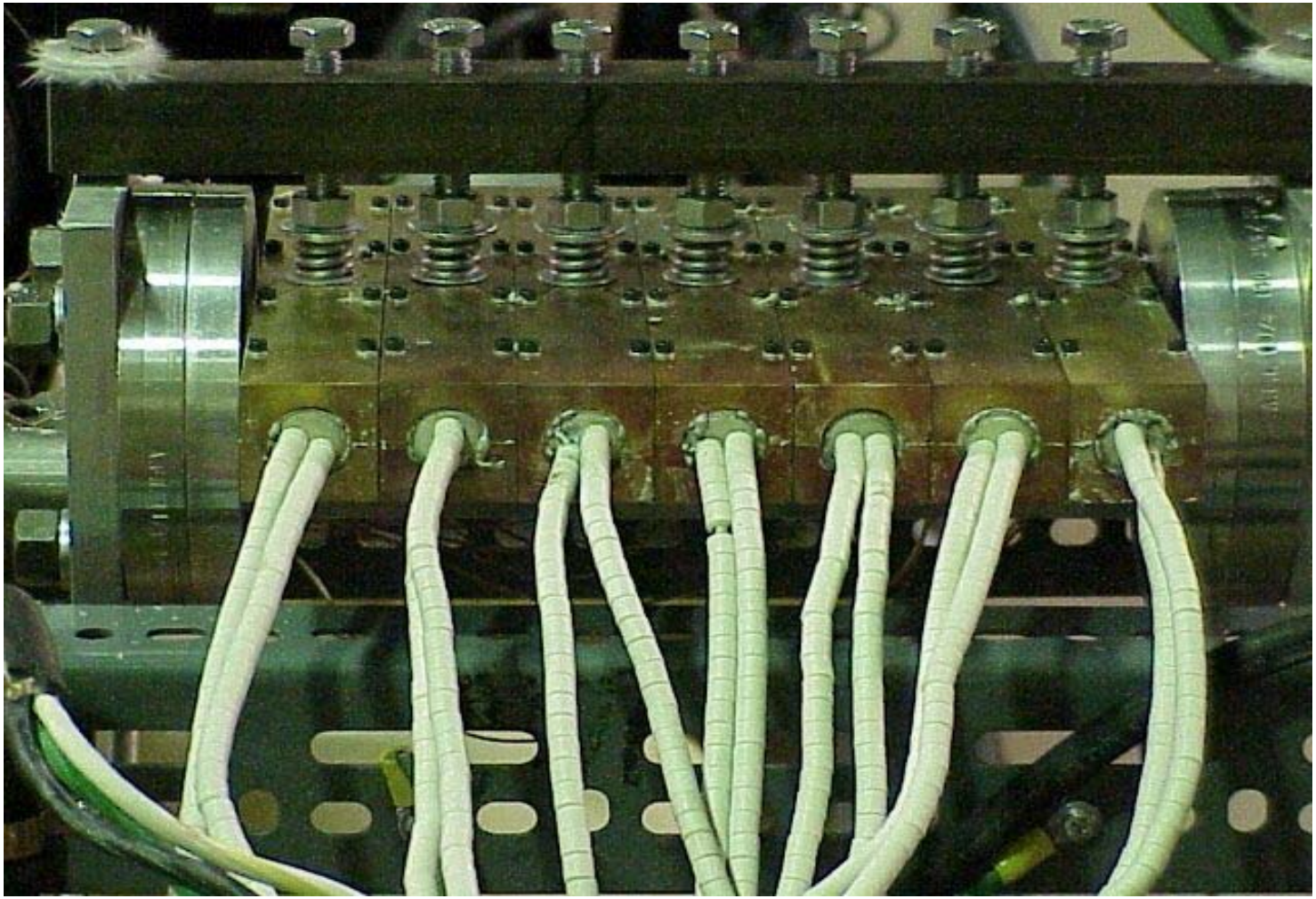

Fig.28 Experimental microchannel test section-copper blocks-thermocouples assembly

REFERENCES

1) "Boron Neutron Capture Therapy," R. F. Barth, A. H. Soloway, R. G. Fairchild, Cancer Res. 50:1061-1070, 1990.

2) "Boron Neutron Capture Therapy for Cancer: Realities and Prospects," R. F. Barth, A. H. Soloway, R. G. Fairchild, R. M. Brugger, Cancer, 70:2995-3001, 1992.

3) "Evaluation of BCNU and or Radiation Therapy in the Treatment of Anaplastic Gliomas (a cooperative clinical trial)", M.D. Walker, E. Alexander and W. Hunt, J. Neurosurg, 49: 333-343, 1978.

4) "Recursive Partitioning Analysis of Progosnotic Factors in Three Radiation Therapy Oncology Group Malignant Glioma Trials," W.J. Curran, C.B. Scott, J. Horton, J.S.Nelson, A.S. Weinstein, A.J. Fischbach, C.H. Chang, M. Rotman, S.O.Asbell, R.E.Krisch, D.F. Nelson, J. National Cancer Institute, 85: 704-710, 1993.

5) "A Neutron Spectrometer for Neutrons with Energies Between 1 eV and 10 keV," C. K. Wang and T. E. Blue, Nucl. Instr. and Meth.A, 290, 237-241 (1990).

6) "A Neutron Spectrometer for Neutron Energies Between 1 eV and 10 keV," C. K. Wang and T. E. Blue, Trans. Am. Nucl. Soc. 57, 79-80 (1988).

7) "An Experimental Study of the Moderator Assembly for a Low-Energy Proton Accelerator Neutron Irradiation Facility for BNCT," C. K. Wang, T. E. Blue, and J. W. Blue, in Neutron Beam Design, Development and Performance for Neutron Capture Therapy , Edited by O. K. Harling, John A. Bernard, and R. G. Zamenhof (Plenum Press, 1990) pp 271-280.

8) "Effect of Head Size on ^{10}B and $^{1}H(n,g)^{2}H$ Dose Distribution for a Broad Field Accelerator Epithermal Neutron Source for BNCT," N. Gupta, J. Niemkiewicz, T. E. Blue, R. A. Gahbauer, and T. X. Qu, Medical Physics 20: 395-404 (1993).

9) "Effect of Head Size on ^{10}B Dose Distribution for a Broad Field Accelerator Epithermal Neutron Source for BNCT," N. Gupta, T. E. Blue, C. Kanellitsas, and R. Gahbauer, Proceedings of Inter. Workshop on Macro and Microdosimetry and Treatment Planning for Neutron Capture Therapy, Boston Oct. 31-Nov. 1, 1991 (in Topics in Dosimetry and Treatment Planning for Neutron Capture Therapy, edited by R. G. Zamenhof, G. R. Solares and O. K. Harling, Advanced Medical Publishing, Madison, WI, 1994) pp. 165-174.

10) "Effect of Head Size on ^{10}B Dose Distributions," N. Gupta, T. E. Blue, Trans. Am. Nucl. Soc. 65, 157-158 (1992) (invited).

11) "Analysis of Flow and Heat Transfer Characteristics of an Asymmetrical Flat Plate Heat Pipe," K. Vafai, W. Wang, International Journal of Heat and Mass Transfer, 35, 2087-2099 (1992).

12) "Development and Evaluation of a Neutron-Gamma Mixed-Field Dosimetry System Based on a Single Thermoluminescence Dosimeter," K. R. Herminghuysen and T. E. Blue, Nucl. Instr. and Meth. A353, 420-424 (1994).

13) "Conceptual Design of an RFQ Accelerator-Based Neutron Source for Boron Neutron Capture Therapy," T. P. Wangler, J. E. Stovall, T. S. Bhatia, C. K. Wang, T. E. Blue, R. A. Gahbauer, Los Alamos National Laboratory article LA-UR-89-912, 1989 Particle Accelerator Conference, Chicago, IL, March 20-23 (1989).

14) "Shielding Design of the Treatment Room for an Accelerator Neutron Source for BNCT," J. F. Evans and T. E. Blue, Proc. of First Inter. Workshop on Accelerator-Based Neutron Sources for Boron Neutron Capture Therapy, Jackson, WY, Sep. 11-14, 1994 (submitted Sep. 1994).

15) "Design and Shielding of a Beam Transport System for Use in an Accelerator-Based Epithermal Neutron Source for BNCT." M. C. Dobelbower, T. E. Blue and R. W. Garnett, Proc. of First Inter. Workshop on Accelerator-Based Neutron Sources for Boron Neutron Capture Therapy, Jackson, WY, Sep. 11-14, 1994 (submitted October 1994).

16) Blue, T. E., Woollard, J. E. and Gupta, N., "Neutron RBE as a Function of Energy," Proceedings of the 8th Inter. Conf. on Rad. Shielding, Amer. Nuc. Soc., La Grange Park, IL, 888-892, (1994).

17) P.R. Gavin, S. L. Kraft, R. Huiskamp and J. A. Coderre, "A Review: CNS Effects and Normal Tissue Tolerance in Dogs", *J. Neuro-Oncol.*, 33, 71-80, (1997).

18) "Photon, Electron, Proton and Neutron Interaction Data for Body Tissues", ICRU 46, International Commission on Radiological Units and Measurements, (1992).

19) Woollard, JE, Blue, TE, Gupta, N and Gahbauer, RA, "Development and Application of Neutron Field Optimization Parameters for an Accelerator-Based Neutron Source for Boron Neutron Capture Therapy", Nucl. Tech. 1996; 155:100-112.

20) N. Gupta, R. A. Gahbauer, T. E. Blue and A. Wambersie, "Dose Prescription in Boron Neutron Capture Therapy," International Journal of Radiation Oncology, Biology and Physics 28:1157-1166 (1994).

21) A. Gahbauer, R. G. Fairchild, J. H. Goodman and T. E. Blue, "RBE in Normal Tissue Studies," Boron Neutron Capture Therapy: Toward Clinical Trials of Glioma Treatment, D. Gabel and R. Moss (ed), Plenum Press, N.Y., 123-128 (1992).

22) J. F. Briesmeister (ed.), "MCNP--A General Monte Carlo N-particle Transport Code, Version 4A," LA-12625, Los Alamos National Laboratory (1993).

23) H. Frankhauser and P. R. Gavin, “Summing Up: Clinical Papers”, in Advances in Neutron Capture Therapy, A. H. Soloway, R. F. Barth and D. E. Carpenter (ed), Plenum Press, N.Y., 799-805, (1993).

24) A. D. Chanana, "Boron Neutron Capture Therapy of Glioblastoma Multiforme at the Brookhaven Medical Research Reactor A Phase I/II Study Protocol #4", January 2, (1996).

25) M. T. Orr, T. E. Blue, and J. E. Woollard, “Using DORT to improve the moderator assembly design for the OSU accelerator-based neutron source for boron neutron capture therapy,” Proc. Embedded Topl. Mtg. Accelerator Applications/Accelerator Driven Transmutation Technology and Applications '01, Reno, NV, November 11-15, 2001, Am. Nucl. Soc. (2001) (CD-ROM).

26) “Optimizing the OSU-ABNS Moderator Assembly Geometry for BNCT,” B. Khorsandi, T.E. Blue, Eleventh World Congress on Neutron Capture Therapy (ISNCT-11), Boston, MA, Oct. 11-15, 2004, CD ROM.

27) I.G. Zubal, C.R. Harrel, E.O. Smith and A.L. Smith, “Two dedicated software voxelbased, anthropomorphic (torso and head) phantoms,” *Proceedings of the International Workshop,* National Radiological Protection Board, Chilton, UK, on 6 and 7 July 1995, pp.105-111 (1996).

28) .F. Evans, T.E. Blue and N. Gupta, “Absorbed dose estimates to structures of the brain and head using a high-resolution voxel-based head phantom,” *Med. Phys.* 28(5), pp.780-786, (2001).

29) M. Cristy and K.F. Eckerman, “Specific Absorbed Fractions of Energy at Various Ages from Internal Photon Sources. I. Methods,” *Oak Ridge National Laboratory,*ORNL/TM-8381/V1 (1987).

30) “The ORNL mathematical phantom series,” http://homer.ornl.gov/vlab/mird2.pdf (1996)

31) International Commission on Radiation Units and Measurements, “Photon Electron, Proton and Neutron Interaction Data for Body Tissues,” ICRU Report 46, (1992).

32) Gupta, N. "Fabrication and Preliminary Testing of a Moderator Assembly for an Accelerator-Based Neutron Source for Boron Neutron Capture Therapy", Ph.D. Dissertation, The Ohio State University, (1995).

33) Gupta, N., Blue, T. E., Dobelbower, M. C., “Preliminary testing of a moderator assembly prototype for an accelerator-based neutron source for BNCT,” Abstracts of the 7th International Symposium on Neutron Capture Therapy for Cancer, Zurich, Switzerland, September, 1996.

34) M. C. Dobelbower, “An Integrated Design of an Accelerator-Based Neutron Source for Boron Neutron Capture Therapy,” Ph.D. Dissertation, The Ohio State University, 1995.

35) P. W. Benjamin, C. D. Kemshall, A. Brickstock, “The Analysis of Proton Recoil Spectra”, United Kingdom Atomic Energy Authority, AWRE Report No. 09/68.

36) C. D. Kenshall, “The Use of Spherical Proportional Counters for Neutron Spectrum Measurements,” AWRE Report No. 031/73.

37) Glidcop is a registered trademark of OMG Americas Corp, Research Triangle Prak, N.C., USA

GRADUATE DEGREES EARNED

DEGREES COMPLETED, M.S. Students

1. Michael C. Dobelbower, Spring 1993, "Improvements in a ^{3}He-based Neutron Spectrometer for Boron Neutron Capture Therapy."

2. Kevin R. Herminghuysen, Summer 1993, "Development and Evaluation of a Neutron-Gamma Mixed-Field Dosimetry System Based on a Single Thermoluminescence Dosimeter."

3. Jeffrey F. Evans, Summer 1994, "Shielding Design of the Treatment Room for an Accelerator Neutron Source for BNCT."

4. Megan L. Gillen, Summer 1995, "A Study of Radiation Transport in BNCT in an Ellipsoidal Water Phantom Using Removal-Diffusion Theory for the Brookhaven Medical Research Reactor Epithermal Beam."

5. Lance Rakovan, Summer 1996, "Neutron Dosimetry Using Aqueous Solutions of Lithium Acetate."

6. Angela S. Brown, Summer 1996, "Using MCNP4A to Model a High Purity Germanium Detector."

7. Michael Reed, July, 1997, "Determination of the Absorbed Dose from an Accelerator-Based Neutron Source for Boron Neutron Capture Therapy using the Paired Ion Chamber Technique"

8. Albert Vest, September 1997, "Thermal Neutron Flux Measurements in an Anthropomorphic Brain Phantom"

9. Lacramiora G. Cotlet , 1998, "Biomathematical Model Of Radiation Induced Bone Marrow Damage"

10. Kinga Krobl , 1999," TLD-700 as Mixed(Thermal Neutron-Gamma) Field Dosimeter"

11. J. Eric Denison, 2000, "Evaluation and Adaptation of an Aqueous Coumarin Dosimeter for Use in Mixed Neutron-Gamma Radiation Fields"

12. Cristian Marciulescu, "Design of the Target Heat Removal System for an Accelerator-Based Neutron Source for Boron Capture Neutron Therapy," NE Program, December 2002; presently employed with Westinghouse Electric Corporation in Pittsburgh, PA.

13. Andrew Hawk, "A Shielding Design for an Accelerator Based Neutron Source for Boron Neutron Capture Therapy", January 2003, NE Program, Cook Nuclear Power Plant, Michigan.

14. Chenguang Li, "A Moderator Assembly Evaluation Method for an ABNS for Boron Neutron Capture Therapy Based on Absorbed Dose Calculations Using a High-resolution Voxel-based Head Phantom", NE Program, Co-Advisor, Nilendu Gupta, August 2003, currently pursuing Ph.D. in Economics at Indiana University.

15. Behrooz Khorsandi, "Material and Geometry Considerations in the Design of a Moderator Assembly for an ABNS for BNCT," NE, 2004, currently in Ph.D. program.

16. Josh Sroka, "Examination of a Delimiter Design for an ABNS for BNCT," NE, Winter 2005, Currently employed at Bettis Atomic Power Lab, Pittsburgh, PA.

DEGREES COMPLETED, Ph.D. Students

1. Tanxia Qu, June 1993, "A Monte Carlo Design Study of an Accelerator Epithermal Neutron Irradiation Facility for Boron Neutron Capture Therapy."

2. Nilendu Gupta, Sept. 1995, "Fabrication and Preliminary Testing of a Moderator Assembly for an Accelerator-Based Neutron Source for Boron Neutron Capture Therapy".

3. John Niemkiewicz, Ph.D. student in Biomedical Engineering, June, 1996, "Radiation Therapy Treatment Planning for an Accelerator Source of Neutrons for Boron Neutron Capture Therapy.

4. Jeffrey E. Woollard, June 1997, "Optimization of a Moderator Assembly for Use in an Accelerator-Based Neutron Source for Boron Neutron Capture Therapy".

5. Michael Christian Dobelbower, December 1997, "An Integrated Design of an Accelerator-Based Neutron Source for Boron Neutron Capture Therapy".

6. Nanqiang Zhu, Ph.D., Summer 1997, "An Analytical and Numerical Investigation of Asymmetrical Disk-Shaped and Flat-Plate Heat Pipes."

7. Yanmin Wang, Ph.D., Summer 1999, "An Experimental and Analytical Investigation of the Transient Characterization of Flat Plate Heat Pipes"

PROJECT RELATED PUBLICATIONS

Papers Published in High Level Technical Journals

1. "Effect of Head Size on ^{10}B and $^{1}H(n,\gamma)^{2}H$ Dose Distribution for a Broad Field Accelerator Epithermal Neutron Source for BNCT," N. Gupta, J. Niemkiewicz, T. E. Blue, R. A. Gahbauer, and T. X. Qu, Medical Physics 20: 395-404 (1993).

2. "A Calculation of the Energy Dependence of the RBE of Neutrons," T. E. Blue, N. Gupta and J. E. Woollard, Physics of Medicine and Biology 38: 1693-1712 (1993).

3. "Dose Prescription in Boron Neutron Capture Therapy," N. Gupta, R. A. Gahbauer, T. E. Blue and A. Wambersie, International Journal of Radiation Oncology, Biology and Physics 28:1157-1166 (1994).

4. "Development and Evaluation of a Neutron-Gamma Mixed-Field Dosimetry System Based on a Single Thermoluminescence Dosimeter," K. R. Herminghuysen and T. E. Blue, Nucl. Instr. and Meth. A353, 420-424 (1994).

5. "An Expression for the RBE of Neutrons as a Function of Neutron Energy," T. E. Blue, J. E. Woollard, N. Gupta and J. F. Greskovich, Jr., Physics of Medicine and Biology 40: 757-767 (1995).

6. "Development and Application of Neutron Field Optimization Parameters for an Accelerator- Based Neutron Source for Boron Neutron Capture Therapy," J.E. Woollard, T.E. Blue, N.Gupta, R.A. Gahbauer, Nuclear Tech., 115, 100-113 (1996).

7. "Shielding Design of a Treatment Room for an Accelerator-Based Epithermal Neutron Irradiation Facility for BNCT," J. F. Evans and T. E. Blue, Health Physics, 71 (5), 692-699 (1996).

8. "The Rationale and Requirements for the Development of Boron Neutron Capture Therapy of Brain Tumors," A. L. Soloway, R. F. Barth, R. A. Gahbauer, T. E. Blue, and J. H. Goodman, Journal of Neuro-Oncology, **33**,9-18(1997).

9. "BNCT: Status and dosimetry requirements," R. Gahbauer, N. Gupta, T. E. Blue, J. Goodman, J. Grecula, A. H. Soloway, A. Wambersie, Radiation Protection Dosimetry, **70**(1-4):547-554 (1997).

10. "Boron Neutron Capture Therapy: Principles and Potential," R. Gahbauer, N. Gupta, T. Blue, J. Goodman, R. Barth, J. Grecula, A. H. Soloway, W. Sauerwein and A. Wambersie, Recent Results in Cancer Research **150**, 183-209(1998).

11." Evaluation of Moderator Assemblies for use in an Accelerator–Based Neutron Source for Boron Neutron Capture Therapy", J.E. Woollard, T.E. Blue, N.Gupta, R.A. Gahbauer, Nuclear Tech. 123, 320-334 (1998)

12 “Neutron Dosimetry In Boron Neutron Capture Therapy Using Aqueous Solutions Of Lithium Acetate”, L.J. Rakovan, T.E. Blue, and A.L. Vest, Nucl. Instr. and Meth.A 414, 357-364(1998).

13. “ Mixed- Field Dosimetry Measurement of a Target Assembly for an Accelerator-based Neutron Source for Boron Neutron Capture Therapy,” M. K. Reed, M. C. Dobelbower, J. E. Woollard, T. E. Blue, Nucl. Instr. and Meth. A 419, 160-166 (1998).

14. “Experimental Verification of In-phantom Calculations for an Accelerator–based Neutron Source for Boron Neutron Capture Therapy,” M. C. Dobelbower, A. Vest, M. K. Reed, T. E. Blue, Medical Physics **26,** 376-380(1999).

15.”Boron Neutron Capture Therapy of Brain Tumors: An Emerging Therapeutic Modality”, R. F. Barth, A. H. Soloway, J. H. Goodman, R.A. Gahbauer, N. Gupta, T.E. Blue, W. Yang, and W Tjarks, Neurosurgery **44** ,433-451(1999).

16. "A Stochastic Model of Radiation Induced Bone Marrow Damage" G. Cotlet and T. E. Blue, Health Physics 78, 289-294(2000).

17."Predictions of a Stochastic Model of Bone Marrow Cell Survival in High Dose Rate Radiation Fields with Arbitrary Neutron to Gamma-Ray Absorbed Dose Rate Ratios", Thomas E. Blue, Jeffrey E. Woollard, Medical Physics 27, 2385-2392(2000)

18.“A Comparison of Neutron Beams for BNCT Based on In-Phantom Neutron Field Assessment Parameters”, J.E. Woollard, B.J. Albertson, M.K. Reed, T.E. Blue, J. Capala, N. Gupta and R.A. Gahbauer, Medical Physics, 28, 184-193(2001)

19."Absorbed Dose Estimates to Structures of the Brain and Head Using a High Resolution Voxel-Based Head Phantom" J.F. Evans, T.E. Blue, and N. Gupta, Medical Physics, 28 , 780-786 (2001)

20."Development and Calculation of an Energy Dependent Normal Brain Tissue Neutron RBE for Evaluating Neutron Fields for BNCT," J.E. Woollard, T.E. Blue, N.Gupta, R.A. Gahbauer, Health Physics, 80. 583-589(2001).

21."An Investigation on the Use of Removal-Diffusion Theory for BNCT Treatment Planning: A Method for Determining Proper Removal-Diffusion Parameters", B. J. Albertson, T.E. Blue, and J. Niemkiewicz, Medical Physics, 28, 1898-1904 (2001).

22.“Accelerator-Based Epithermal Neutron Source for Boron Neutron Capture Therapy of Brain Tumors”, T.E. Blue and J.C. Yanch, Journal of Neuro-Oncology, 62: 19-31 (2003).

23. “Common Challenges and Problems in Clinical Trials of Boron Neutron Capture Therapy of Brain Tumors,” N. Gupta, R.A. Gahbauer, T.E. Blue, and B. Albertson, Journal of Neuro-Oncology 62: 197-210 (2003) .

24. “A Shielding Design for an Accelerator-Based Neutron Source for Boron Neutron Capture Therapy,” A.E. Hawk, T.E.Blue, J.E. Woollard, Applied Radiation and Isotopes, 61:1027-1031 (2004).

25. “Boron Neutron Capture Therapy of Cancer: Current Status and Future Prospects,” R. Barth, J. Coderre, M. Graca, H. Vincente, and T. Blue, Clin Cancer Res 2005;11(11) 3987-4002, June 1, 2005.

26. Zhu, N. and Vafai, K., "Optimization of Asymmetrical Disk-Shaped Heat pipes" AIAA Journal of Thermophysics and Heat Transfer, 10, 179-182 (1996).

27. Zhu, N. and Vafai, K., "The Effects of Liquid-Vapor Coupling and Non-Darcian Transport on Asymmetrical Disk-Shaped Heat pipes" International Journal of Heat and Mass Transfer, 39, 2095-2113 (1996).

28. Vafai, K., Zhu, N. and Wang, W., "Analysis of Asymmetric Disk-Shaped and Flat Plate Heat Pipes" ASME Journal of Heat Transfer, 117, 209-218 (1995).

29. Zhu, N. and Vafai, K., "Numerical and Analytical Investigation of Vapor Flow in a Disk-Shaped Heat Pipe Incorporating Secondary Flow" In press for International Journal of Heat and Mass Transfer.

30. Zhu, N., and Vafai, K., "Vapor and Liquid Flow in an Asymmetrical Flat Plate Heat Pipe-A Three Dimensional Analytical and Numerical Investigation" In Press for International Journal of Heat and Mass Transfer.

31. Vafai, K. and Zhu, N. "Thermal Design and Optimization of a Heat Pipe for Medical Applications" International Conference in Porous Media and Their Applications in Science, Engineering and Industry, ICPM-Vol. 2, Kona, Hawaii (6/96).

32. "Numerical and Analytical Investigation of Vapor Flow in a Disk-Shaped Heat Pipe Incorporating Secondary Flow," Zhu, N., Vafai, K., International Journal of Heat and Mass Transfer,40, 2887-2900 (1997).

33. "The Effects of Liquid-Vapor Coupling and Non-Darcian Transport on Asymmetrical Disk-Shaped Heat pipes," Zhu, N., Vafai, K., International Journal of Heat and Mass Transfer ,39, 2095-2113 (1996).

34. "Optimization of Asymmetrical Disk-Shaped Heat pipes," Zhu, N., Vafai, K., AIAA Journal of Thermophysics and Heat Transfer,10, 179-182 (1996).

35. "Vapor and Liquid Flow in an Asymmetrical Flat Plate Heat Pipe-A Three Dimensional Analytical and Numerical Investigation," Zhu, N., Vafai, K., International Journal of Heat and Mass Transfer (In Press).

36. “Boron Neutron Capture Therapy of Cancer,” Encyclopedia of Medical Devices and Instrumentation, R.F. Barth, J.A. Coderre, M. Graca, H. Vincente, and T. E. Blue, , edited by John Webster, John Wiley & Sons, Inc., Hoboken, New Jersey. Work in progress 2005.

REFEREED PROCEEDINGS:

1. "A Study of a Proton Accelerator System as a Source of Epithermal and Thermal Neutrons at Fluence Rates Characteristic of Reactor Beams," T. E. Blue, J. W. Blue, C. K. Wang, and T. X. Qu, Proc. Seventh ASTM-EURATOM Symposium on Reactor Dosimetry, Strasbourg, France, August 1990, edited by G. Tsotridis, R. Dierckx, P. D'Hondt (Kluwer Academic Publishers, Dordrecht, Netherlands 1992) pp. 885-890.

2. "An Integrated Neutronic and Thermal-Hydraulic Design Study for an Accelerator Neutron Irradiation Facility," T. E. Blue, T. X. B. Qu, R. Christensen, P. Guo, J. W. Blue, Proceedings Fourth International Symposium on Neutron Capture Therapy for Tumors, Sydney, Australia, Dec. 4-7, 1990 (in Progress in Neutron Capture Therapy for Cancer Edited by B. J. Allen, D. E. Moore and B. V. Harrington, Plenum Press, 1992) pp 113-117.

3. "Proposed Clinical Approach to BNCT," R. A. Gahbauer, R. G. Fairchild, J. H. Goodman, T. E. Blue, Proceedings Fourth International Symposium on Neutron Capture Therapy for Tumors, Sydney, Australia, Dec. 4-7, 1990 (in Progress in Neutron Capture Therapy for Cancer, edited by B. J. Allen, D. E. Moore and B. V. Harrington, Plenum Press, 1992) pp 589-591.

4. "Can Relative Biological Effectiveness be used for Treatment Planning in Boron Neutron Capture Therapy?" R. Gahbauer, R. Fairchild, T. Blue, Advanced Radiation Therapy: Tumor Response Monitoring and Treatment Planning, International Symposium, Munich, Germany, April 11-13, 1991, In: Advanced Radiation Therapy Tumor Response Monitoring and Treatment Planning, Editor A. Breit, Springer-Verlag, Berlin/Heidelberg, pp. 755-758 (1992).

5. "RBE in Normal Tissue Studies," R. A. Gahbauer, R. G. Fairchild, J. H. Goodman, T. E. Blue, Proc. European Collaboration on Boron Neutron Capture Therapy, Petten, in Boron Neutron Capture Therapy, Ed. D Gable and R. Moss, Plenum Press, N.Y., pp. 123-128 (1992).

6. "Point Kernel 1H(n,gamma)2H Dose Calculations in BNCT," J. Niemkiewicz, N. Gupta, T. E. Blue, Trans. Am. Nucl. Soc. 65,155-157 (1992) (invited).

7. "Effect of Head Size on 10B Dose Distributions," N. Gupta, T. E. Blue, Trans. Am. Nucl. Soc. 65, 157-158 (1992) (invited).

8. "Monte Carlo Analysis of an Accelerator Epithermal Neutron Irradiation Facility (AENIF) for Boron Neutron Capture Therapy," T. E. Blue, T. X. B. Qu, N. Gupta, R. Gahbauer, in Proceedings of ANS Meeting New Horizons in Radiation Protection and Shielding, April 26-May 1, 1992 Richland, WA. pp 75-79 (1992) (invited).

9. "Monte Carlo Shielding Analysis for an Accelerator Epithermal Neutron Irradiation Facility (AENIF) in a Conventional X-Ray Irradiation Room," T. Qu, E. Blue, K. Herminghuysen, C. Kanellitsas, R. Gahbauer, Advances in Neutron Capture Therapy, Editied by A.H. Soloway et al., Plenum Press, New York, 115-118 (1993).

10. “Effect of Variations in the RBE on the Design of an AENIF for BNCT,” T. E. Blue, T. X. B. Qu, N. Gupta, R. Gahbauer, Advances in Neutron Capture Therapy: Proceedings of 5th Inter. Symp. on Neutron Capture Therapy, Columbus, OH. Sept. 1992, Plenum Publishing, NY, pp. 99-103 (1993).

11. “Monte Carlo Shielding Calculations of an Accelerator Neutron Irradiation Facility for Boron Neutron Capture Therapy,” T. X. Qu, T. E. Blue, C. Kanellitsas and R. A. Gahbauer, Advances in Neutron Capture Therapy: Proceedings of 5th Inter. Symp. on Neutron Capture Therapy, Columbus, OH. Sept. 1992, Plenum Publishing, NY, pp. 115-118 (1993).

12. “Removal-Diffusion Theory for Calculation of Neutron Distributions in BNCT,” J. Niemkiewicz and T. E. Blue, Advances in Neutron Capture Therapy: Proceedings of 5th Inter. Symp. on Neutron Capture Therapy, Columbus, OH. Sept. 1992, Plenum Publishing, NY, pp. 177-180 (1993).

13. “Calculation of Gamma Dose from $^{1}H(n,\gamma)^{2}H$ Interactions in BNCT,” J. Niemkiewicz, N. Gupta, T. E. Blue, in Proceedings of Inter. Workshop on Macro and Microdosimetry and Treatment Planning for Neutron Capture Therapy, Boston Oct. 31-Nov. 1, 1991 (in Topics in Dosimetry and Treatment Planning for Neutron Capture Therapy, edited by R. G. Zamenhof, G. R. Solares and O. K. Harling, Advanced Medical Publishing, Madison, WI, 1994) pp. 157-164.

14. “Effect of Head Size on 10B Dose Distribution for a Broad Field Accelerator Epithermal Neutron Source for BNCT,” N. Gupta, T. E. Blue, C. Kanellitsas, and R. Gahbauer, Proceedings of Inter. Workshop on Macro and Microdosimetry and Treatment Planning for Neutron Capture Therapy, Boston Oct. 31-Nov. 1, 1991 (in Topics in Dosimetry and Treatment Planning for Neutron Capture Therapy, edited by R. G. Zamenhof, G. R. Solares and O. K. Harling, Advanced Medical Publishing, Madison, WI, 1994) pp. 165-174.

15. “Neutron RBE as a Function of Energy,” T. E. Blue, J. E. Woollard and N. Gupta, Proceedings of 8th Inter. Conf. on Radiation Shielding, Arlington, TX, April, 1994, pp. 888-892 (1994).

16. “Calculations of Neutron Flux Distributions in BNCT using Removal-Diffusion Theory,” J. M. Niemkiewicz, T. E. Blue and N. Gupta, Trans. Am. Nucl. Soc.70: 13-15 (1994) (invited).

17. “A Calculation of the Neutron RBE for Boron Neutron Capture Therapy,” T. E. Blue, J. E. Woollard and N. Gupta, Trans. Am. Nucl. Soc 70: 17-19 (1994) (invited).

18. “Prediction of Normal Tissue Response in Boron Neutron Capture Therapy,”N. Gupta, R.A. Gahbauer, T.E. Blue, Proceedings of the 16th International Cancer Congress, New Delhi, India, November 1994, R. S. Rao, M. G. Deo, L.D. Sanghvi, and I. Mittra, eds., Monduzzi Editore, Bologna, Italy, pp. 669-673 (1994).

19. “Engineering and Practical Considerations for Fabrication of a Moderator Assembly for an Accelerator Neutron Source for BNCT,” N. Gupta, T. E. Blue and J. W. Blue, Proc. of First Inter. Workshop on Accelerator-Based Neutron Sources for Boron

Neutron Capture Therapy, Jackson, WY, Sep. 11-14, 1994 , INEL Report Conference-940976, pp. 311-326 (1995)

20. "Shielding Design of the Treatment Room for an Accelerator Neutron Source for BNCT," J. F. Evans and T. E. Blue, Proc. of First Inter. Workshop on Accelerator-Based Neutron Sources for Boron Neutron Capture Therapy, Jackson, WY, Sep. 11-14, 1994, INEL Report Conference-940976, pp. 441-458 (1995).

21. "Beam Design and Evaluation for BNCT," T. E. Blue, J. E. Woollard, N. Gupta and R. A. Gahbauer, Proc. of First Inter. Workshop on Accelerator-Based Neutron Sources for Boron Neutron Capture Therapy, Jackson, WY, Sep. 11-14, 1994, INEL Report Conference-940976, pp. 197-212 (1995).

22. "Optimization of a Moderator Assembly for Use in an Accelerator-Based Epithermal Neutron Source for BNCT," J. E. Woollard, T. E. Blue and N. Gupta, Proc. of First Inter. Workshop on Accelerator-Based Neutron Sources for Boron Neutron Capture Therapy, Jackson, WY, Sep. 11-14, 1994 , INEL Report Conference-940976, pp. 327-340 (1995).

23. "Design and Shielding of a Beam Transport System for Use in an Accelerator-Based Epithermal Neutron Source for BNCT." M. C. Dobelbower, T. E. Blue and R. W. Garnett, Proc. of First Inter. Workshop on Accelerator-Based Neutron Sources for Boron Neutron Capture Therapy, Jackson, WY, Sep. 11-14, 1994, INEL Report Conference-940976, pp. 99-110 (1995).

24. "Shielding Design of a Treatment Room for an Accelerator-Based Neutron Source for BNCT," J.F. Evans and T.E. Blue, Trans. Am. Nucl. Soc. 72: 306-307 (1995).

25. "Neutron Capture Therapy: Its Potential as a Therapeutic Modality in Radio-Oncology," A. Soloway, R. Barth, R. Gahbauer, T.E. Blue, J. Goodman, Proceedings of the 5th International Meeting on Progress in Radio-Oncology JCRO/ÿGRO5 Salzburg, Austria, May 10-14, 1995. In Progress in Radio-Oncology V H.D. Kogelnik, ed. Monduzzi Editore, Bologna, Italy pp. 309-314 (1995).

26. "Neutron Field Optimization Parameters for Boron Neutron Capture Therapy," J.E. Woollard, N. Gupta, T.E. Blue, R.A. Gahbauer, Trans. Am. Nucl. Soc. 73: 25-26 (1995).

27. "BNCT: A promising area of research?", Gahbauer, R., Gupta, N., Blue, T., Goodman, J., Grecula, J., Soloway, A. H., Wambersie, A Proceedings of the 5th International Conference on Applications of Nuclear Techniques: "Neutrons in Research and Industry", Crete, Greece (1996), SPIE Proceedings Series Vol 2867, p 12-22 (1997) (invited).

28. "A Monte Carlo Analysis of the Effect of Increasing Target Diameter for an Accelerator-Based Neutron Source for BNCT," Dobelbower, T. E. Blue, Proc. Topical Meeting on Nuclear Applications of Accelerator Technology, Albuquerque, NM, Nov. 1997, pp 495-501(1997).

29. “Effect of Duty Factor and Repetition Rate on Maximum Target Temperature for a Proposed BNCT Target Assembly,” Dobelbower, T. E. Blue, K. Vafai, Proc. Topical Meeting on Nuclear Applications of Accelerator Technology, Albuquerque, NM, Nov. 1997,pp 516-520(1997).

30. “A Calculation of and Sensitivity Study for Neutron RBEs for BNCT”, J.E. Woollard and T.E. Blue, in Advances in Neutron Capture Therapy - Volume I, Medicine and Physics, B. Larsson, J. Crawford and R. Weinreich, (eds.), pp. 253-258(1997)

31. “Clinical Significance of In-Phantom Evaluation Parameters for Epithermal Neutron Beams in BNCT,” N. Gupta, R. Gahbauer, T. E. Blue, J. Woollard in Advances in Neutron Capture Therapy - Volume I, Medicine and Physics, B. Larsson, J. Crawford and R. Weinreich, (eds.), pp. 264-270 (1997)

32. “The Use of Removal-Diffusion Theory to Calculate Neutron Flux Distributions for Dose Determination in Boron Neutron Capture Therapy,” J. Niemkiewicz, T. E. Blue in Advances in Neutron Capture Therapy - Volume I, Medicine and Physics, B. Larsson, J. Crawford and R. Weinreich, (eds.), pp. 275-278 (1997)

33. “Fractionation in BNCT: what are the issues? R. Gahbauer, N. Gupta, T. E. Blue, J. Grecula, J. Goodman, A. Wambersie, Advances in Neutron Capture Therapy - Volume II, Chemistry and Biology, B. Larsson, J. Crawford and R. Weinreich, (eds.), pp.683-686(1997)

34. “An In–Phantom Comparison of Neutron Fields for BNCT,” J.E. Woollard, T.E. Blue, and J . Capala, Trans. Am. Nucl. Soc. 78, 15-17 (1998).(invited)

35. Absorbed Dose Estimates with a High-Resolution Voxel-Based Head Phantom," J.F. Evans and T.E, Blue, Trans. Am. Nucl. Soc. 78, 5-6 (1998).(invited)

36. "Stochastic Model of Radiation Induced Bone Marrow Toxicity Applied to Criticality Accident Scenario" G. Cotlet, T. E. Blue and W. E. Carey, Trans. Am. Nucl. Soc. 80, 135-137(1999)

37. "Ion Chamber Dosimetry for an ABNS for BNCT,” M. K. Reed, M. C. Dobelbower, J. E. Woollard, T. E. Blue, Trans. Am. Nucl. Soc. 80, 70-71 (1999).(invited)

38. “A Comparison of Neutron Beams for BNCT,” T.E. Blue and J.E. Woollard, Trans. Am. Nucl. Soc. 84, 121-123, (2001).(invited)

39. “Calculation Of Absorbed Dose Distributions Using Removal Diffusion Theory For BNCT Treatment Planning,” B. J. Albertson, J. Niemkiewicz, T. E. Blue, and N. Gupta, Frontiers in Neutron Capture Therapy, Proceedings of Eighth Inter. Symp. on Neutron Capture Therapy for Cancer, La Jolla, CA, Sept. 1998 M. F. Hawthorne, K. Shelly, and R. J. Wiersema (ed), Plenum, pp.683-686, (2001)

40. "Absorbed Dose Estimates with a High Resolution Voxel-Based Head Phantom" J.F. Evans and T.E, Blue, Frontiers in Neutron Capture Therapy, Proceedings of Eighth Inter. Symp. on Neutron Capture Therapy for Cancer, La Jolla, CA, Sept. 1998 M. F. Hawthorne, K. Shelly, and R. J. Wiersema (ed), Plenum, pp.605-609, (2001)

41. “A Comparison Of Neutron Fields For BNCT,” J.E. Woollard, T.E. Blue, and J . Capala, Frontiers in Neutron Capture Therapy, Proceedings of Eighth Inter. Symp. on Neutron Capture Therapy for Cancer, La Jolla, CA, Sept. 1998 M. F. Hawthorne, K. Shelly, and R. J. Wiersema (ed), Plenum, pp.413-417, (2001)

42. "Reporting a BNCT Irradiation," R. Gahbauer, N. Gupta, T. Blue, D. Carpenter, W. Sauerwein, and A. Wambersie, Frontiers in Neutron Capture Therapy, Proceedings of Eighth Inter. Symp. on Neutron Capture Therapy for Cancer, La Jolla, CA, Sept. 1998 M. F. Hawthorne, K. Shelly, and R. J. Wiersema (ed), Plenum, pp.565-569, (2001)

43. "Treatment Plan Evaluation in Boron Neutron Capture Therapy," N. Gupta, R.A. Gahbauer, and T.E. Blue, Frontiers in Neutron Capture Therapy, Proceedings of Eighth Inter. Symp. on Neutron Capture Therapy for Cancer, La Jolla, CA, Sept. 1998 M. F. Hawthorne, K. Shelly, and R. J. Wiersema (ed), Plenum, pp.201-206, (2001)

44. “ Using DORT to Improve the Moderator Assembly Design for the OSU Accelerator-Based Neutron Source for Boron Neutron Capture Therapy,” M. T. Orr, T. E. Blue, J. E. Woollard, Proceedings of the Embedded Topl. Mtg. Accelerator Applications/Accelerator Driven Transmutation Technology and Applications ’01, Reno, NV, Nov. 11-15, 2001, Am. Nucl. Soc (CD-ROM).

45. “Design of the Heat Removal System for BNCT Therapy”, C. Marciulescu, T. E. Blue, J. E. Woollard, Trans. Am. Nucl. Soc. 86 (2002)

46. “Effects of Target Thickness on Neutron Field Quality for an ABNS for BNCT”, A. E. Hawk, T. E. Blue, J. E. Woollard, Trans. Am. Nucl. Soc. 86 (2002)

47. “Effects of Target Thickness on Neutron Field Quality for an ABNS,” A. Hawk, T.E. Blue, J. Woollard, N. Gupta, Research and Development in Neutron Capture Therapy, Proceedings of 10th Inter. Congress. on Neutron Capture Therapy, Essen, Germany, Sept. 2002, Wolfgang Sauerwein, Raymond Moss, Andrea Wittig (ed), Monduzzi Editore, pp.253-257, (2002)

48. “Material Considerations in the Design of a Moderator Assembly for an ABNS for BNCT,” B. Khorsandi, T.E. Blue, N. Gupta, J.E. Woollard, A.E. Hawk, Trans. Am. Nucl. Soc. 87 (2002)

49. “A Comparison of Field Quality for an Accelerator-Based Neutron Source and an Idealized Standard Reactor Neutron Field for BNCT,”T.E. Blue, A.E. Hawk, J.E. Woollard, Trans. Am. Nucl. Soc. 87 (2002)

50. “Impact of ABNS Moderator Assembly Geometry on BNCT Neutron Field,” B. Khorsandi, T.E. Blue, C. Li, A. Hawk, Accelerator Applications for a Nuclear Renaissance, San Diego, CA, 6/1/03-6/5/03. Trans. Am. Nucl. Soc. 88 (June 2003), pg.478-483.

51. "Dynamic Thermal Performance Analysis of a Target and Heat Removal System for an Accelerator-Based Neutron Source for Boron Neutron Capture Therapy," T.E. Blue, B. Khorsandi, Accelerator Applications for a Nuclear Renaissance, San Diego, CA, 6/1/03-6/5/03. Trans. Am. Nucl. Soc. 88 (June 2003) pg.178-183.

52. "Dose Distributions in BNCT Using a Structure-Segmented Head Phantom," C. Li, T.E. Blue, N. Gupta, Trans. Am. Nucl. Soc. 89 (November 2003).

53. "Field Assessment in BNCT Using a Structure-Segmented Head Phantom," C. Li, T.E. Blue, N. Gupta, Trans. Am. Nucl., Vol. 90, Pittsburgh, PA (June, 2004), 328-329.

54. "Optimizing the OSU-ABNS Base Moderator Assembly Materials for BNCT," B. Khorsandi, T. Blue, Eleventh World Congress on Neutron Capture Therapy (ISNCT-11), Boston, MA, Oct. 11-15, 2004, CD ROM.

55. "Field Assessment Using a Structure-segmented Head Phantom," C. Li, T.E. Blue, N. Gupta, Eleventh World Congress on Neutron Capture Therapy (ISNCT-11), Boston, MA, Oct. 11-15, 2004, CD ROM.

56. "Moderator Assembly Design Assessment Using Newly-designed Neutron Field Assessment Parameters," C. Li, T.E. Blue, N. Gupta, Eleventh World Congress on Neutron Capture Therapy (ISNCT-11), Boston, MA, Oct. 11-15, 2004, CD ROM.

57. "Optimizing the OSU-ABNS Moderator Assembly Geometry for BNCT," B. Khorsandi, T.E. Blue, Eleventh World Congress on Neutron Capture Therapy (ISNCT-11), Boston, MA, Oct. 11-15, 2004, CD ROM.

58. "Design of a Moderator Assembly Delimiter for an ABNS for BNCT," J. Sroka, T. Blue, C. Li, A. Hawk, and N. Gupta, American Nuclear Society, The Monte Carlo Method: Versatility Unbounded in a Dynamic Computing World, Chattanooga, TN, April 17-21, 2005

59. "MCNP Model of the Semiconductor Device Characterization Vessel in BP1 of the OSURR ," J. Sroka, T. Blue, A. Kauffmann, Transactions Vol.93, ANS 2005 Winter Meeting, November 13-15, 2005, Washington DC, on CD-ROM, pp 603-604 .

OTHER PUBLICATIONS/PROCEEDINGS/ABSTRACTS:

1. "Monte Carlo Shielding Calculations of an Accelerator Neutron Irradiation Facility for Boron Neutron Capture Therapy," T. B. Qu, T. E. Blue, and R. A. Gahbauer, Proceedings Health Phys. Soc. Annual Meeting, Columbus, OH. June 1992 Health Physics 62, S28-29 (1992).

2. "Improvements on a ^{3}He Based Neutron Spectrometer," M. C. Dobelbower, G. Shani, and T. E. Blue, Proceedings Health Phys. Soc. Annual Meeting, Columbus, OH. June 1992 Health Physics 62, S6 (1992).

3. "Macro-Microdosimetry, RBE-Compound Factor, Geometrical Dose Distribution: What Do We Need to Establish Tolerance Limits?" R. A. Gahbauer, J. Grecula, J. H. Goodman, T. E. Blue and R. Fairchild, Abstracts of Fifth Inter. Symp. on Neutron Capture Therapy for Cancer, Columbus, OH. Sept. 1992; p. 33 (1992).

4. "Effect of Variations in the RBE on the Design of an AENIF for BNCT," T. E. Blue, T. X. B. Qu, N. Gupta, R. A. Gahbauer and J. W. Blue, Abstracts of Fifth Inter. Symp. on Neutron Capture Therapy for Cancer, Columbus, OH. Sept. 1992; p. 46 (1992).

5. "A Measurement of CHF on Vertical Surface in Natural Convective Boiling System for BNCT," R. N. Christensen, P. Guo and T. E. Blue, Abstracts of Fifth Inter. Symp. on Neutron Capture Therapy for Cancer, Columbus, OH. Sept. 1992; p. 48 (1992).

6. "Monte Carlo Shielding Calculations of an Accelerator Neutron Irradiation Facility for Boron Neutron Capture Therapy," T. X. Qu, T. E. Blue, C. Kanellitsas and R. A. Gahbauer, Abstracts of Fifth Inter. Symp. on Neutron Capture Therapy for Cancer, Columbus, OH. Sept. 1992; p. 48 (1992).

7. "A Study on the Effect of Head Size on ^{10}B Dose Distributions," N. Gupta, T. E. Blue and R. A. Gahbauer, Abstracts of Fifth Inter. Symp. on Neutron Capture Therapy for Cancer, Columbus, OH. Sept. 1992; p. 71 (1992).

8. "Removal-Diffusion Theory for Calculation of Neutron Distributions in BNCT," J. Niemkewicz and T. E. Blue, Abstracts of Fifth Inter. Symp. on Neutron Capture Therapy for Cancer, Columbus, OH. Sept. 1992; p. 72 (1992).

9. "Calculation of the Gamma Dose Distribution in BNCT by the Point Kernel Method," J. Niemkewicz, N. Gupta and T. E. Blue, Abstracts of Fifth Inter. Symp. on Neutron Capture Therapy for Cancer, Columbus, OH. Sept. 1992; p. 78 (1992).

10. "Analysis of Compounds with Respect to Expected Therapeutic Gain in Boron Neutron Capture Therapy," R. A. Gahbauer, J. Grecula, T. E. Blue, N. Gupta, J. Goodman, B. Laster, International Congress of Radiation Oncology 1993, Kyoto, Japan, June, 1993.

11. "Development and Evaluation of a Neutron-Gamma Mixed-Field Dosimetry System Based on a Single Thermoluminescence Dosimeter," K. R. Herminghuysen and T. E. Blue, 1994 Symp. on Radiation Measurements and Applications, Ann Arbor, MI, May 16 – 19, 1994.

12. "Design and Shielding of a Beam Transport System for use in an Accelerator Neutron Source for BNCT," M. C. Dobelbower, T. E. Blue and R. W. Garnett, Abstract Compendium for First Inter. Workshop on Accelerator-Based Neutron Sources for Boron Neutron Capture Therapy, Jackson, WY, Sep. 11-14, 1994, p. 8 (1994).

13. "Design of a Disk Shaped Target for the Heat Removal Process in a BNCT Application," N. Zhu, K. Vafai and T. E. Blue, Abstract Compendium for First Inter. Workshop on Accelerator-Based Neutron Sources for Boron Neutron Capture Therapy, Jackson, WY, Sep. 11-14, 1994, p. 17 (1994).

14. "Beam Design and Evaluation for BNCT," T. E. Blue, J. E. Woollard, N. Gupta and R. A. Gahbauer, Abstract Compendium for First Inter. Workshop on Accelerator-Based Neutron Sources for Boron Neutron Capture Therapy, Jackson, WY, Sep. 11-14, 1994, p. 22 (1994).

15. "Engineering and Practical Considerations for Fabrication of a Moderator Assembly for an Accelerator Neutron Source for BNCT," N. Gupta, T. E. Blue and J. W. Blue, Abstract Compendium for First Inter. Workshop on Accelerator-Based Neutron Sources for Boron Neutron Capture Therapy, Jackson, WY, Sep. 11-14, 1994, p.43 (1994).

16. "Optimization of a Moderator/Reflector Assembly for use in an Accelerator Based Epithermal Neutron Source for BNCT," J. E. Woollard, T. E. Blue and N. Gupta, Abstract Compendium for First Inter. Workshop on Accelerator-Based Neutron Sources for Boron Neutron Capture Therapy, Jackson, WY, Sep. 11-14, 1994, p. 45 (1994).

17. "Preconceptual Shielding Design of the Treatment Room for an Accelerator Neutron Source for BNCT," J. F. Evans and T. E. Blue, Abstract Compendium for First Inter. Workshop on Accelerator-Based Neutron Sources for Boron Neutron Capture Therapy, Jackson, WY, Sep. 11-14, 1994, p.68 (1994).

18. "An Accelerator Neutron Source for BNCT," T. E. Blue, K. Vafai, R. A. Gahbauer, M. C. Dobelbower, J. F. Evans, N. Gupta and J. E. Woollard, Abstracts of Boron Neutron Capture Therapy Contractor/Grantee Workshop, U. S. Department of Energy, Office of Energy Research, Office of Health and Environmental Research, Germantown, NY, Oct. 13, 1994 (invited).

19. "Prediction of Normal Tissue Response in BNCT," N. Gupta, R. A. Gahbauer, T. E. Blue, J. Grecula, PSBT1-19, Abstract Book I, XVI International Cancer Congress, New Delhi, Nov. 1994, pp. 257.

20. Evans and T. E. Blue, Proceedings of Health Physics Soc. Annual Meeting, Boston, MA, July 1995, Health Physics 68, S35 (1995).

21. "Design of an Accelerator-Based Epithermal Neutron Source for BNCT", C. Dobelbower, T. E. Blue, K. Vafai, R. Gahbauer, N. Gupta, and J. Woollard, Proceedings 16th Annual Conference on Medical Physics, Jodhpur, India, Nov. 8-10, 1995.

22. "Effect of Target Size on an Expression for the Energy Dependent RBE of Low Energy Neutrons," J. E. Woollard, T. E. Blue, N. Gupta, Rad. Research Soc. 44th Annual Mtg., Chicago, Ill. April, 1996.

23. “The Use of Removal-Diffusion Theory to Calculated Neutron Distribution for Dose Determination in Boron Neutron Capture Therapy,” J. Niemkiewicz and T. E. Blue, Abstracts of Seventh Inter. Symp. on Neutron Capture Therapy for Cancer, Zurich, Switzerland, Sept. 1996.

24. “Design of an Accelerator-Based Epithermal Neutron Source for BNCT,” T. E. Blue, M. C. Dobelbower, K. Vafai, R. A. Gahbauer, N. Gupta, J. E. Woollard, Abstracts of Seventh Inter. Symp. on Neutron Capture Therapy for Cancer, Zurich, Switzerland, Sept. 1996.

25. “Predicted Effect of Recombination on the Energy Dependence of an Expression for an RBE of Low-Energy Neutrons,” T. E. Blue, J. E. Woollard and N. Gupta, Abstracts of Seventh Inter. Symp. on Neutron Capture Therapy for Cancer, Zurich, Switzerland, Sept. 1996.

26. “A Target Assembly Cooling Design for a BNCT Application,” N. Zhu, K. Vafai, C. P. Desai and T. E. Blue, Abstracts of Seventh Inter. Symp. on Neutron Capture Therapy for Cancer, Zurich, Switzerland, Sept. 1996.

27. “Fractionation in BNCT: What are the Issues,” R. A. Gahbauer, N. Gupta, J. Grecula, T. E. Blue, and A. Wambersie, Abstracts of Seventh Inter. Symp. on Neutron Capture Therapy for Cancer, Zurich, Switzerland, Sept. 1996.

28. “Clinical Significance of In-phantom Evaluation Parameters for Epithermal Neutron Beams in BNCT,” N. Gupta, R. A. Gahbauer, T. E. Blue, J. Woollard, Abstracts of Seventh Inter. Symp. on Neutron Capture Therapy for Cancer, Zurich, Switzerland, Sept. 1996.

29. “Preliminary Testing of a Moderator Assembly Prototype for an Accelerator-Based Neutron Source for Boron Neutron Capture Therapy,” N. Gupta, T. E. Blue, M. C. Dobelbower, Abstracts of Seventh Inter. Symp. on Neutron Capture Therapy for Cancer, Zurich, Switzerland, Sept. 1996.

30. “Design of an Accelerator-Based Epithermal Neutron Source for BNCT,” T. E. Blue, C. Dobelbower, N. Gupta, J. Woollard, Proceedings of the 56th Annual Meeting of the Ohio State Radiological Society, Columbus, OH, May 11, 1996.(invited)

31. "An Accelerator-based Epithermal Neutron Source for Boron Neutron Capture Therapy", T. E. Blue, M. C. Dobelbower, J.E. Woollard, N. Gupta, K. Vafai, R.A. Gahbauer, Abstracts of Third Topical Mtg on Industrial Radiation and Radioisotope Measurements and Applications, p18, Raleigh, NC(1996)

32. “BNCT: A Promising Area of Research?,” R. Gahbauer, N. Gupta, T. E. Blue, J. Goodman, J. Grecula, A. H. Soloway, A. Wambersie, Proceedings of the 5th International Conference on Applications of Nuclear Techniques: “Neutrons in Research and Industry,” Crete, Greece, (1996).

33. “Accelerator design requirements for a hospital-based BNCT facility,” Gupta, N., Blue, T.E., Vafai, K., Gahbauer, R. A., Dobelbower, M.C., Woollard, J. E., Abstracts

for the Fourteenth International Conference on the Application of Accelerators in Research and Industry, Denton, Texas, Nov 1996 (invited).

34."A Sensitivity Analysis of an Expression for Energy Dependent RBEs of Low Energy Neutrons", J.E. Woollard, T.E. Blue , Proc. of Radiation Research Society 45th Annual Meeting, Providence, RI, May 3-7, 1997, pg 217 (1997).

35."A New Dose Prescription For BNCT That Includes Volume Effects", J. F. Evans, N. Gupta and T.E. Blue, Proc. of Radiation Research Society 456th Annual Meeting, Louisville, KY, April 25-30, 1998, pg (1998).

36."Biomathematical Model Of Radiation Induced Bone Marrow Toxicity For Various Radiation Protocols", L.G. Cotlet, T. E. Blue and W. Carey, Proc. of Radiation Research Society 46th Annual Meeting, Louisville, KY, April 25-30, 1998, pg (1998).

37. "TLD-700 as A Mixed Field Dosimeter", K. Krobl , M.C. Dobelbower and T. E. Blue"

38. "Treatment Plan Evaluation in BNCT," N. Gupta, R. Gahbauer, T. E. Blue, A. Wambersie, Abstracts of Eighth Inter. Symp. on Neutron Capture Therapy for Cancer, La Jolla, CA, Sept. 1998, p.159(1998)

39. "Reporting of BNCT Irradiation: Application of The ICRU Recommendations To The Situation In BNCT," R. Gahbauer, N. Gupta, T. E. Blue, W.Sauerwein, and A. Wambersie, Abstracts of Eighth Inter. Symp. on Neutron Capture Therapy for Cancer, La Jolla, CA, Sept. 1998, pp.102-103(1998).

40. "A Comparison of Neutron Fields For BNCT," J.E. Woollard, T.E. Blue, and J . Capala, Abstracts of Eighth Inter. Symp. on Neutron Capture Therapy for Cancer, La Jolla, CA, Sept. 1998, p.71(1998)

41. "Experimental Verification Of In-Phantom Calculations For An Accelerator-Based Neutron Source For Boron Neutron Capture Therapy," M. C. Dobelbower, A. Vest, M. K. Reed, T. E. Blue, Abstracts of Eighth Inter. Symp. on Neutron Capture Therapy for Cancer, La Jolla, CA, Sept. 1998, p.106(1998)

42. "Calculation Of Absorbed Dose Distributions Using Removal Diffusion Theory For BNCT Treatment Planning," B. J. Albertson," J. Niemkiewicz, T. E. Blue, and N. Gupta, Abstracts of Eighth Inter. Symp. on Neutron Capture Therapy for Cancer, La Jolla, CA, Sept. 1998, p.151(1998)

43."Absorbed Dose Estimates with a High Resolution Voxel-Based Head Phantom," J. F. Evans, T. E. Blue, and N. Gupta, Abstracts of Eighth Inter. Symp. on Neutron Capture Therapy for Cancer, La Jolla, CA, Sept. 1998, p.124(1998)

44. "A Comparison of Measurements with Calculations for an Accelerator-Based Neutron Source for BNCT, T. E. Blue, M. C. Dobelbower, M. K. Reed, J.E. Woollard, A. Vest, Abstracts for the Fifteenth International Conference on the

Application of Accelerators in Research and Industry, Denton, Texas, Nov 1998 p.22 (1998) (invited).

45. “A Comparison of Measurements with Calculations for an Accelerator-based Neutron Source for BNCT,” Abstracts of The OSU Comprehensive Cancer Center Scientific Retreat, Newark, OH, Dec.16, 1998, p. 11(1998).

46. “Absorbed Dose Estimates with a High-Resolution Voxel-Based Head Phantom,” Abstracts of The OSU Comprehensive Cancer Center Scientific Retreat, Newark, OH, Dec.16, 1998. p. 12(1998).

47. "The Impact of Assumptions Regarding the Effectiveness of Gamma Rays in Controlling Gliomas on an In-Phantom Comparison of Neutron Fields for BNCT," T. E. Blue, J. E. Woollard, R. A. Gahbauer*, N. Gupta*, and Jacek Capala, IAEA Joint Technical Committee Meeting on Research Reactor Utilization for NCT, June 1999 (invited)

48. “Effects of Target Thickness on Neutron Field Quality for an ABNS,” A. E. Hawk, T. E. Blue, J. E. Woollard, Abstracts of Tenth Inter. Symp. on Neutron Capture Therapy for Cancer, Essen, Germany, Sept. 2002.-`-